NASA

Technical Memorandum 86171

A Sphere-Scanning Radiometer for Rapid Directional Measurements of Sky and Ground Radiance: The PARABOLA Field Instrument.

Donald W. Deering
Peter Leone

NOVEMBER, 1984

National Aeronautics and
Space Administration

Goddard Space Flight Center
Greenbelt, Maryland 20771

A SPHERE-SCANNING RADIOMETER FOR RAPID DIRECTIONAL MEASUREMENTS OF SKY AND GROUND RADIANCE: THE PARABOLA FIELD INSTRUMENT

Donald W. Deering
Earth Resources Branch/623
Laboratory for Terrestrial Physics

and

Peter Leone
Experimental Instrumentation Branch/674
Laboratory for Oceans

NASA/Goddard Space Flight Center
Greenbelt, Maryland
20771

November 1984

ABSTRACT

Accurate interpretation and maximum use of multispectral data acquired from spaceborne and aircraft instruments requires increased knowledge and understanding of the bidirectional reflectance characteristics of earth scene elements. The complexities of the angular distribution of bidirectional reflectance from earth terrain surfaces, particularly vegetation, have become more evident from field studies that attempt to advance the state-of-the-art of remote sensing. Currently available field instrumentation, however, has proven inadequate for acquiring multiple viewing angle radiometric measurements of target surfaces in a short enough time period to effectively eliminate the effects of changing solar position, sky conditions and biophysical parameter states or conditions, while coincidentally measuring the distributional characteristics of the complete irradiance field.

A unique new field instrument, called the PARABOLA, has been designed, along with a collapsable support boom, to be self-contained and easily transportable to remote sites to enable the acquisition of radiance data for almost the complete (4π) sky-and ground-looking hemispheres in only 11 seconds. The PARABOLA samples in 15° instantaneous field-of-view sectors in three narrow-bandpass spectral channels (currently filtered for visible, near-infrared and shortwave infrared wavelengths) simultaneously. Laboratory tests and calibrations have been performed, data processing software has been developed, and instrument modifications have been made based on field use evaluations. Field measurement studies have been performed on a variety of earth surface cover types using a truck boom, a specially designed pickup truck mounting system, and a hot air balloon. In addition to

the improved capability for better measurements to understand the nature of the bidirectional reflectance properties of earth cover types, the PARABOLA instrument has obvious potential for climatological and other studies requiring characterization of the distribution of diffuse solar radiation within the sky hemisphere.

CONTENTS

ILLUSTRATIONS

INTRODUCTION

In recent years several studies have clearly shown that plant canopies and other earth terrain surfaces do not reflect the incident solar radiation in an isotropic manner (i.e., Lambertian or scattering radiant energy equally in all directions). Early airborne radiometer measurements of Salomonson (1966) and Salomonson and Marlatt (1968, 1971), which were followed by those of Kriebel (1978) and more recently by Barnsley (1984), all indicate differing reflectance anisotropy over various natural surface types including crops, grassland, forest, bare soil and snow. With aircraft sensor measurements, the angle dependent properties are partly caused by the atmosphere but the major contribution is due to the surface anisotropy (Ott 1984). However, virtually all applications of remotely sensed data (for example, satellite multispectral scanner data) of the earth's surface make the assumption that such surfaces are Lambertian. This assumption can lead to inaccuracies in (or conversely, accounting for anisotropy can improve) image classifications (Smith and Oliver 1974, Ott et al. 1984), computation of the earth radiation budget and climate model predictions from satellite data (King and Curran 1980, Hughes and Henderson-Sellers 1982) and plant canopy model computations for biophysical parameter estimation (Goel et al. 1984). Eaton and Dirmhirn (1979) report that only careful ground measurements provide a means to determine the actual bidirectional reflectance distribution characteristics of natural surfaces and subsequently to determine ground albedo patterns from space data.

Although a large number of field studies of spectral reflectance of vegetation have been conducted, most measurements have been taken

only from a nadir looking view angle. Those field studies that have considered the angular viewing effects, such as Egbert and Ulaby (1972), Colwell (1974), Verhoef and Bunnick (1976), Rao et al. (1979), Kirchner et al. (1982), Ranson et al. (1981) and Kimes (1983) have revealed the complexities of bidirectional reflectance from earth terrain surfaces. Such bidirectional reflectances involve the complicated interactions of viewing angle, solar zenith and azimuth angles, diurnal and multitemporal biophysical parameter changes, and illumination or sky conditions. For example, Kriebel (1976) found that the directional reflected radiation of natural surfaces may change even if nothing except the distribution of the irradiation over the hemisphere varies, while Park and Deering (1984) showed differences in directional plant canopy reflectance with changes in biomass and sun elevation, and Kirchner (1982) reported changes in the directional reflectance that were associated with leaf orientation changes for the same plant canopy.

In early 1980 NASA began conducting a series of four workshops involving approximately 100 scientists from around the United States, to identify those areas where basic research is needed to analytically predict the electromagnetic response of renewable earth resource features considering the surface and atmospheric influence and underlying parameter variability (Smith 1980). The key research issue identified for the optical-reflective regime was the "critical need to obtain spectral measurements of the complete bidirectional reflectance distribution function (BRDF) of scene element classes". In further describing the need they continued that multi-directional measurements must be made "which are insensitive to short term irradiance fluctuations"

and that they "must also include a measurement of the complete irradiance field". A second research issue identified through the workshops was the "need to understand spectral data acquired under hazy or scattered cloud conditions in the field", which carries with it the need to make "concurrent measurement of the downwelling spectral irradiance components (direct and diffuse) and the target upwelling radiance". Thus, the need for detailed studies of the bidirectional reflectance distribution properties of earth scene elements has become apparent, as well as the need for new instruments to meet the directional sky and ground measurement requirements.

Field measurements of a single set of directional reflectance measurements (i.e., approximately 40 angles; e.g., five view angles at eight azimuths) of a ground target using currently available instrumentation typically takes 20 to 30 minutes but may take over an hour depending on the type of instrument used and actual measurements taken (Ranson 1981, Kimes 1983, Vanderbilt et al. 1983). Steven (1977) required 40 minutes to make the 34 angular observations for measuring the radiance distribution of the sky. Consequently, his measurement technique is limited to the clear and completely cloudless case; and of course he obtained no measurement of a ground target during that period of time.

This paper describes a bidirectional reflectance field instrument and the primary associated transportable platform system that were designed and constructed at the NASA Goddard Space Flight Center. The instrument has been field tested, modified, re-evaluated and used in field investigations over two growing seasons.

INSTRUMENT DEVELOPMENT

Design Considerations

Two factors were recognized as primary limitations of existing field instruments for obtaining adequate field measurements to analyze the bidirectional reflectance angular distribution of ground targets. The major instrument limitation was considered to be the difficulty in obtaining multiple viewing angle measurements of the surface target in a very short time period to eliminate, or at least greatly minimize, the effects of changing sun position, sky conditions and the vegetation's dynamic biophysical conditions during the sampling period. Another important limitation was the capability to simultaneously measure the downwelling sky radiance distribution while measuring the ground target.

Five key instrument requirements were specified that bore heavily on the bidirectional reflectance field instrument design. These requirements, developed from the above considerations and the primary author's anticipated use of the instrument, include the following: 1) very rapid sampling (i.e. <30 sec.) of the entire sky and ground target hemispheres in several spectral bands, 2) good radiometric sensitivity (e.g. NE$\Delta\rho$<0.5%) optimized for green vegetation and stability for in situ field measurements ranging from humid to desert environments, 3) a completely self-contained data acquisition system and a large data storage capability to allow extensive sampling at remote sites, 4) completely portable and rugged enough for field use, and 5) a multiple platform mounting capability to allow attaching the radiometer head to a variety of potential support structures to enable measurements over or within a wide range of plant community

types. These key requirements thus defined the new radiometer as a Portable Apparatus for Rapid Acquisition of Bidirectional Observation of the Land and Atmosphere or PARABOLA.

Other important instrument design requirements as originally specified included 1) radiometric spatial sampling of the sky and ground hemispheres in approximately 15° increments for the view zenith angles and approximately 30° increments for view azimuth angles, and 2) spectral sampling in several botanically important wavelength regions with a minimal requirement for a visible red band (e.g., 0.66 μm) and a near-infrared band, (e.g., 0.83 μm), with a shortwave infrared band (e.g., 1.65 μm) considered to be highly desirable.

Development Schedule

Keeping design and development costs of the instrument within a relatively limited budget was an important consideration, and, in fact, the time schedule of instrument design and production was dictated by the somewhat limited and irregular funding available for the effort.

These instrument requirements were first presented by the Goddard Earth Resources Branch scientists to the Goddard engineers in November 1979, and the purchase and fabrication of the PARABOLA components began approximately one year later following design completion. The instrument was assembled for the first time in August and September 1980, and the first field check of the radiometer, as mounted on a tripod, was conducted in November 1981. Modifications were engineered and the first preliminary field use of the PARABOLA was made toward the end of the 1982 growing season using the large tripod mount. The first

field data revealed the absolute necessity for a truck-mounted operation for most of the anticipated target types, and a mount was designed and built for use on the boom-equipped instrument van used in other remote sensing field studies at Goddard. The first full use of the PARABOLA was in the 1983 growing season on pasture and crop lands. With this field experience, a Transportable Pickup Mounting System (TPMS) was designed in the fall to retain the full "portability" requirement for data acquisitions at remote sites. The TPMS was successfully field tested in June 1984 and subsequently modified and enhanced prior to the first major field experiment using the total PARABOLA/TPMS system on rangelands in the semiarid West Texas in September 1984. In addition, a special PARABOLA mount, modified from the van boom mount, was designed and built for use on a hot air balloon to enable data acquisition over forest canopies. This device was successfully used in July 1984 over the mixed forests of Maryland's eastern shore, highlighting the versatility of the PARABOLA instrument system.

Creating an instrument that would look at the same "study plot" or ground target area while measuring the reflected radiance for all view zenith and azimuth directions was desired, but it was recognized that with the aforementioned constraints such an engineering feat might not be practicable. The obvious implication is that the sample target area must be (assumed to be) spatially homogeneous over the range of viewing angles deemed critical to a given study and/or spatial replicate sampling may be required. Thus, efficient mobility was considered critical.

PARABOLA DESCRIPTION AND PERFORMANCE

General Description

The basic PARABOLA instrument is a 3-channel, rotating head radiometer consisting of three primary units--the sensor head, data recording unit, and internal power pack (Figure 1).

The sensor head is composed of a motor-driven two-axis gimbel on which three detector units are jointly mounted. The three detectors

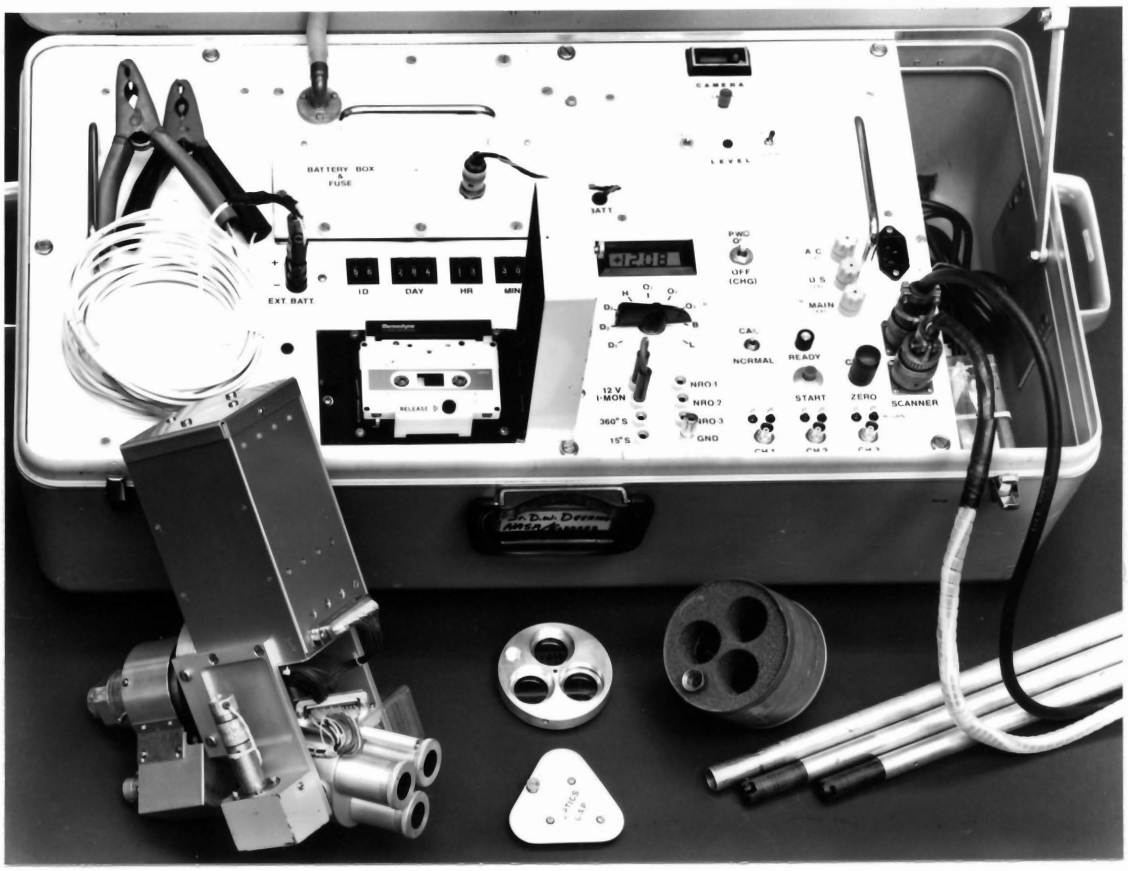

Figure 1. Primary components of PARABOLA including radiometer head and data system box.

include two silicon and one germanium solid state detectors, which are initially configured to correspond with Thematic Mapper spectral bands 3, 4 and 5 (.63-.69 μm, .76-.90 μm, and 1.55-1.75 μm), respectively. The detector cones confine their individual fields of view to 15°. The two-axis, twomotor rotation of the head enables a near-complete sampling of the entire sky/ground sphere. There is a 15° exclusion area toward the mounting device due to mechanical limiations.

The scan system is designed such that sampling is done in a continuous helical pattern. The data is recorded serially in digital form. There is also a "calibrate"/hold position (mode) that allows manual pointing of the detector head for individual measurements of calibration sources in any direction. In the helical sampling mode a complete data set can be taken in only 11 seconds followed by a 35 second data dump to the tape recorder from the buffer. Approximately fifty data sets can be stored on one digital cassette tape. The data recording unit is a small suitcase-sized box (24x 42x80 cm) that weighs 30 kg (65 lbs.) containing the tape recorder, control panel, electronic circuits, rechargeable battery pack, and cable connectors. The sensor's optical head, which weighs 4 kg (8.5 lbs.) is designed with a bayonet-type coupling to enable simple mounting to a variety of potential support devices. The sensor head in its protective carrying case weighs 9 kg (20 lbs.).

Sensor Scan System

The sensor scan head consists of a detector head, an electronics box and two scan motors, one for the roll axis and one for the elevation (or pitch) axis. During use the sensor's scan head is horizontal

(parallel to the ground target to be scanned) and pointing away from the support mount toward the horizon (Figure 2). During the data

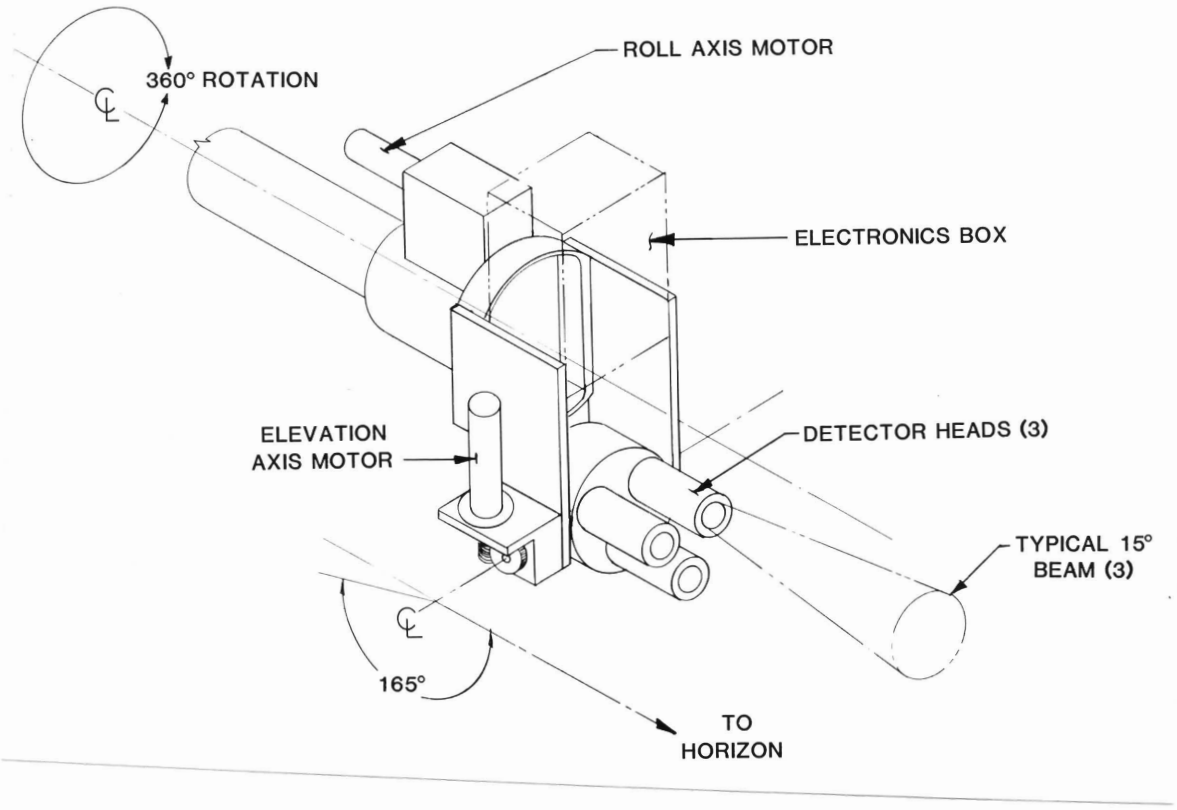

Figure 2. PARABOLA sensor scan head diaghram and rotational characteristics.

acquisition cycle the scan head rotates at 1 RPS about an axis parallel to the head support beam, while at the same time tilting at the rate of 15 deg./sec. about the orthogonal horizontal axis. The roll axis scan rate provides contiguous swaths at the nadir/zenith positions (IFOV is 15°), and progressively increasing overlap at other elevation angles away from the nadir/zenith position. A timing wheel optical sensor triggers concurrent electronic sampling of the radiometric/voltage

outputs from the three detectors at 15° intervals along the roll axis. The resultant radiometric sampling scan procedure results in 264 samples for each channel per scan cycle. The scan pattern produced is depicted in Figure 3. The precise angle of the detector head on the

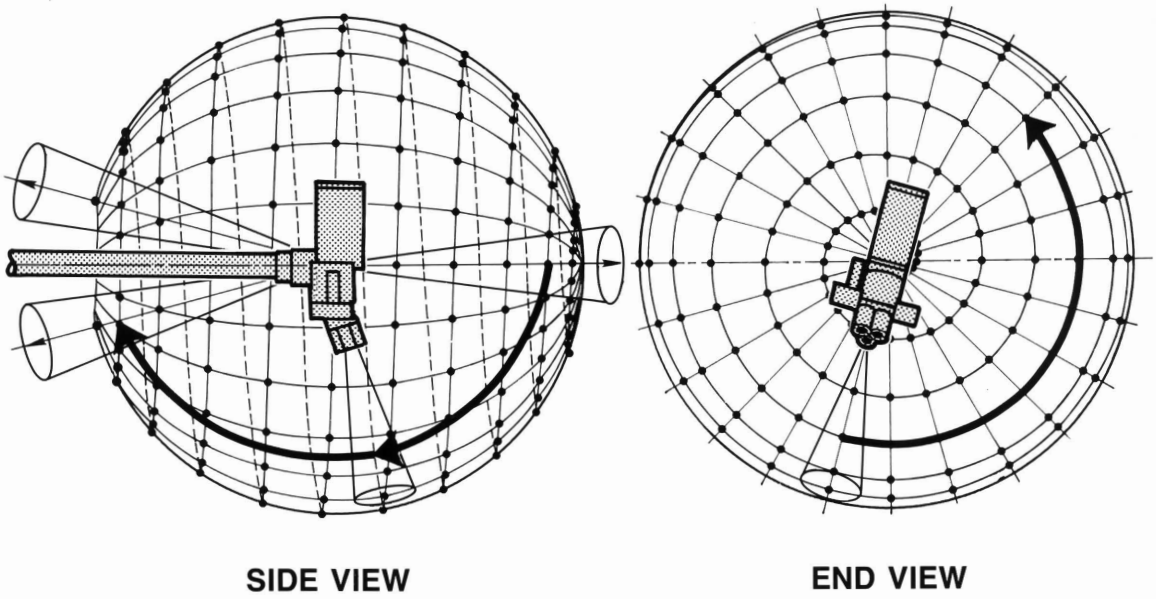

Figure 3. PARABOLA scan pattern in relation to the scan head showing the location of radiometric sampling positions (represented by dots) during the scan cycle.

the elevation axis at the time of each roll-axis-triggered sample is determined from the output of a potentiometer on the elevation axis. (see also Appendix A).

The optics for the detector scan head are a nonrefractive-nonreflective type employing three baffled cones, one for each detector. The "major cone" of detection is 15°, with 4.43° shadowing by design.

Laboratory measurement of the actual optical transfer characteristics of the detector cone assembly are given in Figure 4 for Channel 1.

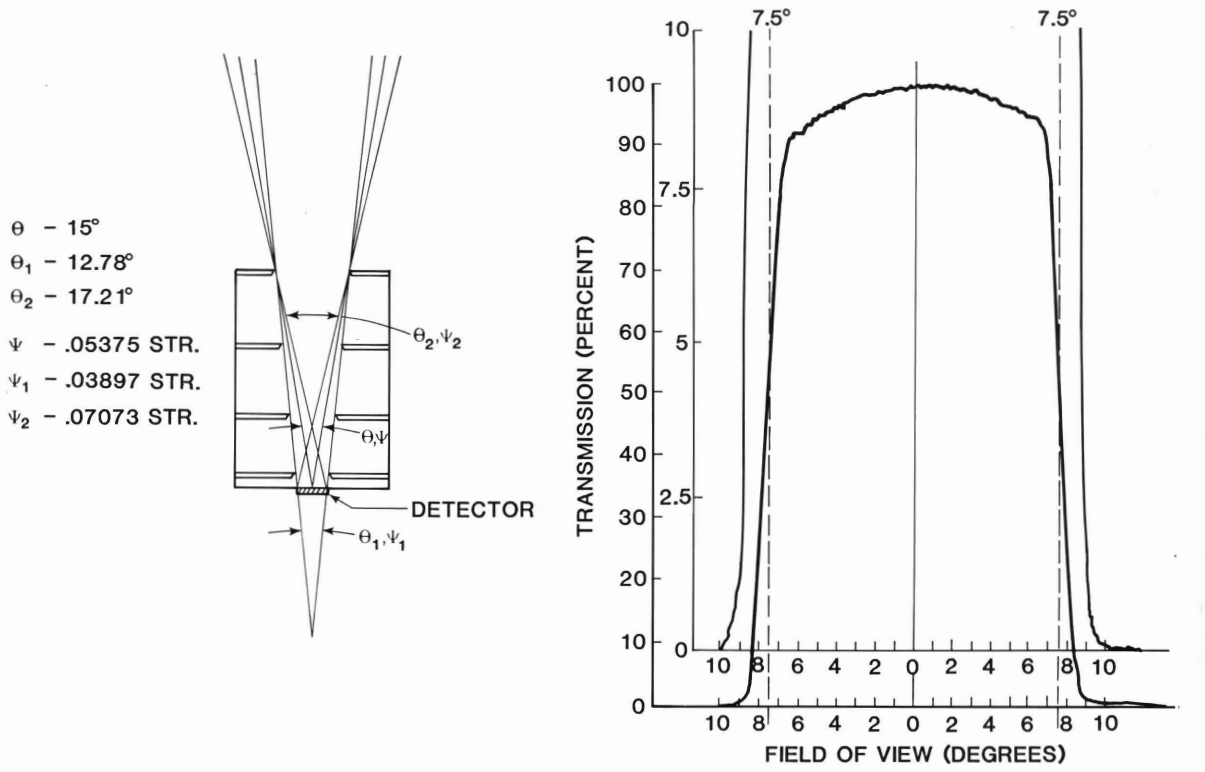

Figure 4. Diagram of baffle cone construction design (left) and field-of-view test results for Channel 1 with cone using a single point source illumination.

Channels 2 and 3 tests show similar results with only slightly greater transmission recorded beyond 9° off-axis at the 0-1% level of transmission.

Two of the three detectors in the PARABOLA radiometer are silicon photodiodes to cover the spectral range from the visible through the near-

infrared. The Channel 3 detector is a germanium photodiode designed to measure the mid-infrared region. The spectral channels are defined by fully blocked narrow band interference filters. The actual (measured) 3 channel wavelength bands (Figure 5), which approximate the Thematic Mapper wavelengths in TM Channels 3, 4 and 5 respectively, are as follows:

Channel	Center Wavelength	Width
1	.6623 µm	.0213 µm
2	.8263 µm	.0295 µm
3	1.658 µm	.068 µm

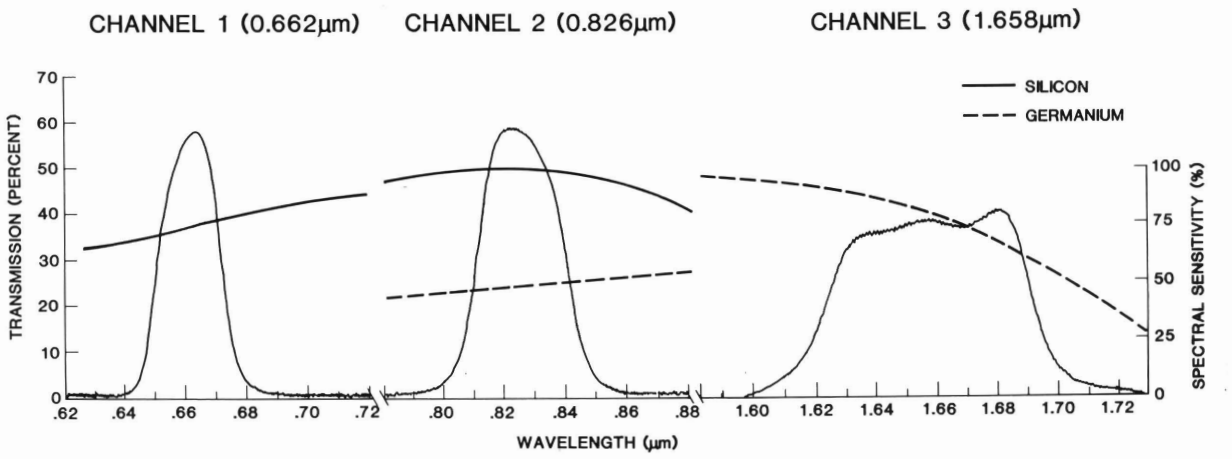

Figure 5. Measured spectral transmission response for the three PARABOLA bandpass filters and relative sensitivities for silicon and germanium detectors.

The detector head is designed such that the spectral bandpass filters can be easily replaced to provide spectral wavelength measurements suited to a particular study (e.g., to match wavebands of a specific satellite such as the AVHRR or French SPOT sensors).

All three detectors are temperature regulated (by cooling or heating) through thermoelectric proportional control circuits. Channels 1 and 2 (silicon) are maintained at 20°±2°C and Channel 3 (germanium) is stabilized to 5°±2°C. Detector temperatures are automatically recorded with each scan data set acquisition. The detector housing temperature, which indicates the ambient environment, is also monitored through an integrated circuit sensor (0 to 100°C range, ±1°C) and recorded automatically. Figure 6 shows the relationship

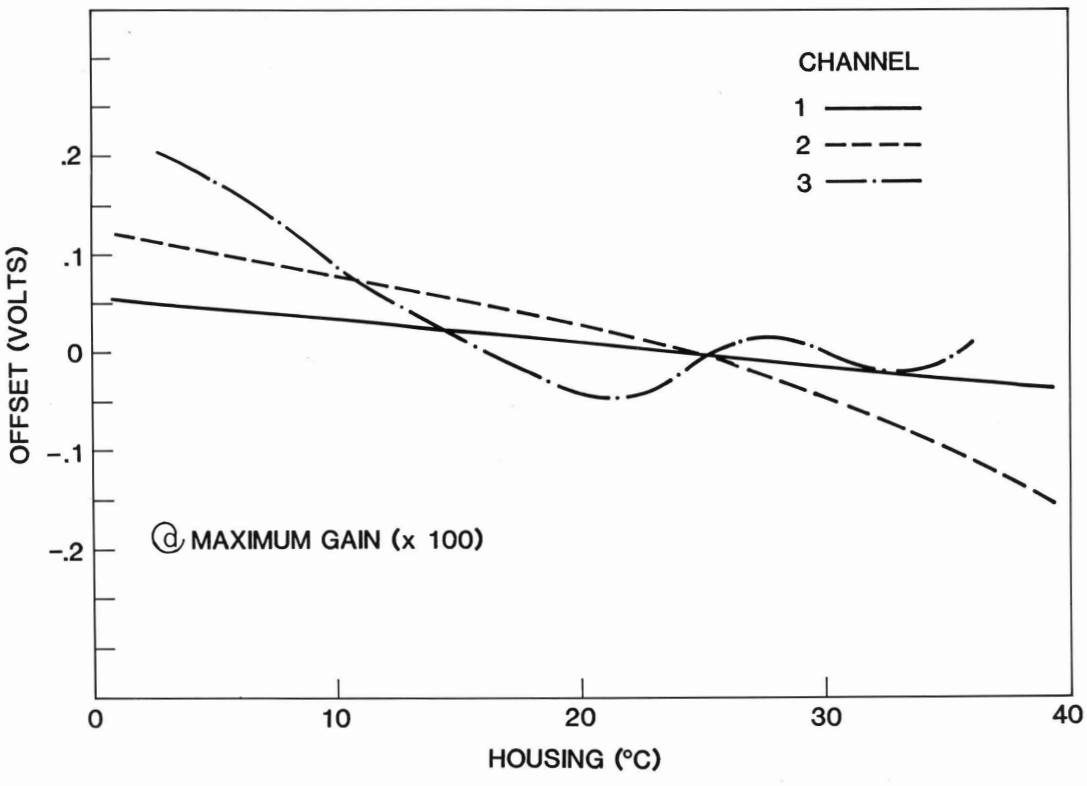

Figure 6. Detector drift relationship to changes in detector housing temperature from simulated environments test.

between the detector housing temperature (simulated environments spanning two extremes) and the resultant voltage offsets measured for each of the three detectors.

The detector gains have been set for high sensitivity to low reflectance readings that are encountered with dense plant canopies and low sun elevations. This has made the zero drift apparent and reaches about 1.5% of full scale on the highest gain range for Channel 2, which it should be noted is only 0.015% of the measurement range, and at extreme (worst-case) ambient temperatures. The noise levels for Channels 1 and 2 are determined primarily by the amplifier, and are well below the quantizing capability of the 10-bit data system. Channel 3 is detector-noise-limited; its noise is about equal to the least significant bit. The PARABOLA noise levels measured with maximum gain, the detectors capped and a bandwidth of 1 Hz to 1 kHz are as follows:

Channel	Output Noise (volts rms)
1	6.25×10^{-4}
2	9.62×10^{-4}
3	9.77×10^{-3}

Channel 1 and Channel 2 drift is quite predictable and can be easily corrected by subtracting measured offsets. Channel 3 drift is seen to be more erratic, but can be precisely zeroed routinely while the sensor is capped by means of a simple gain control on the data system box control panel.

Due to the tremendous range in target brightness that can be expected in scanning a 4π field of view including dark vegetation, bright soil, and bright or dark clouds and sky, an auto-ranging

amplifier is used to switch the gain levels back-and-forth by factors of 1, 10 and 100 to maintain maximum radiometric sensitivity. In addition, since the direct sun brightness is so large and to accurately measure the direct beam radiance would require sacrificing a tremendous amount of sensitivity in the diffuse sky and ground radiances, the three channel gains were set such that saturation results when the PARABOLA views the sun in a normal scan. A neutral density filter cap (see Figure 1) was devised to snap onto the detector baffle cones such that direct solar beam measurements are easily made by manual pin-hole sighting alignment while the data system is set for the "calibrate" mode. Thus, with the temperature controls and monitoring, the Channel 3 manual gain adjustment, and the automatic gain switching, the PARABOLA is well optimized for its intended use.

Data System

The PARABOLA data system is contained within the fiberglass control panel box as seen in Figure 1. The key operation features of the control panel are the digital cassette tape recorder, power switch, scan selector mode switch (normal scan or "calibrate" position), "ready" light and start button, panel meter with readout selector switch (for detector and housing temperatures, detector voltage readings, battery voltage, and scan head leveling angles), header selection switches (to manually preset the data set identification number, day of year, hour of day and minutes), and remote camera switch and frame counter.

The data system samples four channels of analog data (3 from the detectors and 1 from the elevation axis position sensor) simultaneously at every 15° of rotation about the roll axis. The input voltage

ranges from 0-10V and is recorded serially on the digital tape cassette as 8 bit words. The radiometric data resolution is 10 bits, with an accuracy of 0.1% of full scale ±0.5 least significant bit, while the elevation position data is recorded as 8 bits. The data is formatted on the tape in three records as follows: 1) header records, containing two synchronization words and the four presettable header words consisting of data set identification, day, hour, and minutes; 2) data records including gain setting data, elevation position data, scan mode indicator, and detector voltage data; and 3) temperature records, giving the detectors and housing temperatures at the end of each scan. The recording time is approximately 45 seconds per normal scan mode run and about 5 seconds per calibration mode run.

Power System

The primary power supply is a 12 volt, sealed, lead-acid battery rated at 10 ampere-hours which is contained within the control panel box (Fig. 1). The battery is in a sealed box vented only to the outside of the control panel box to minimize the hazard of possible venting of explosive gases. A built-in battery charger operates automatically whenever 115VAC power is connected to the system. Charge time is 20 hours from flat to full, but overnight charging (6-8 hours) has proven sufficient for complete recharging under normal use conditions. Charging (at 1.0 ampere) is indicated by an LED on the control panel, and when full charge is reached, current drops to a trickle level (.03 ampere) and the LED goes out. Three fuses protect the data system and power system components.

Actual field use of the PARABOLA has shown that under some conditions the internal power supply is not adequate. For example,

when sampling is done at frequent intervals over a period of several hours (e.g., sun-up until solar noon) in very hot weather it is desirable to keep the power turned on continuously to keep the detectors cooled and the dark current calibration simple. Power consumption is 1.62A on standby and 2.16A during scanning. Also, when additional power is required, such as with the motorized leveling of the PARABOLA scan head with the Transportable Pickup Mount System (described later), additional battery drain occurs.

Under heavy, long-hours use of the PARABOLA an auxillary external battery connection capability is available. Standard auto battery "jumper cable" spring clamps are attached to a direct-plug-in PARABOLA battery cable approximately 20' long. Thus, the 12V battery of the pickup being used to transport the instrument or a separate, detached auxillary battery can be easily connected to provide a tremendously increased power reserve (e.g. 40-60 ampere-hours). This capability is especially useful if 115VAC power is not available for overnight recharging of the internal battery.

Radiometric Calibration

Radiometric laboratory calibration of the PARABOLA is performed at Goddard on a 1.8 m (72 inch) spherical integrator employing twelve 200-watt quartz halogen lamps (2950°K @ 6.5 amps). The number of lamps illuminating the sphere is varied to produce twelve radiance levels for calibration.

Three separate calibration runs are made to fully calibrate the PARABOLA at the three gain levels. Neutral density filters (.1 and .01 density levels) are used for the two lowest gain settings. The voltage response to radiance level relationship (Figure 7) is linear

in all three spectral channels for each gain setting with linear correlation coefficients of 0.999 (r^2). Calibrations performed after one full year of use and testing (May 1982-May 1983) showed no significant change in voltage output for the same radiance levels, which indicates the stability of the total PARABOLA system.

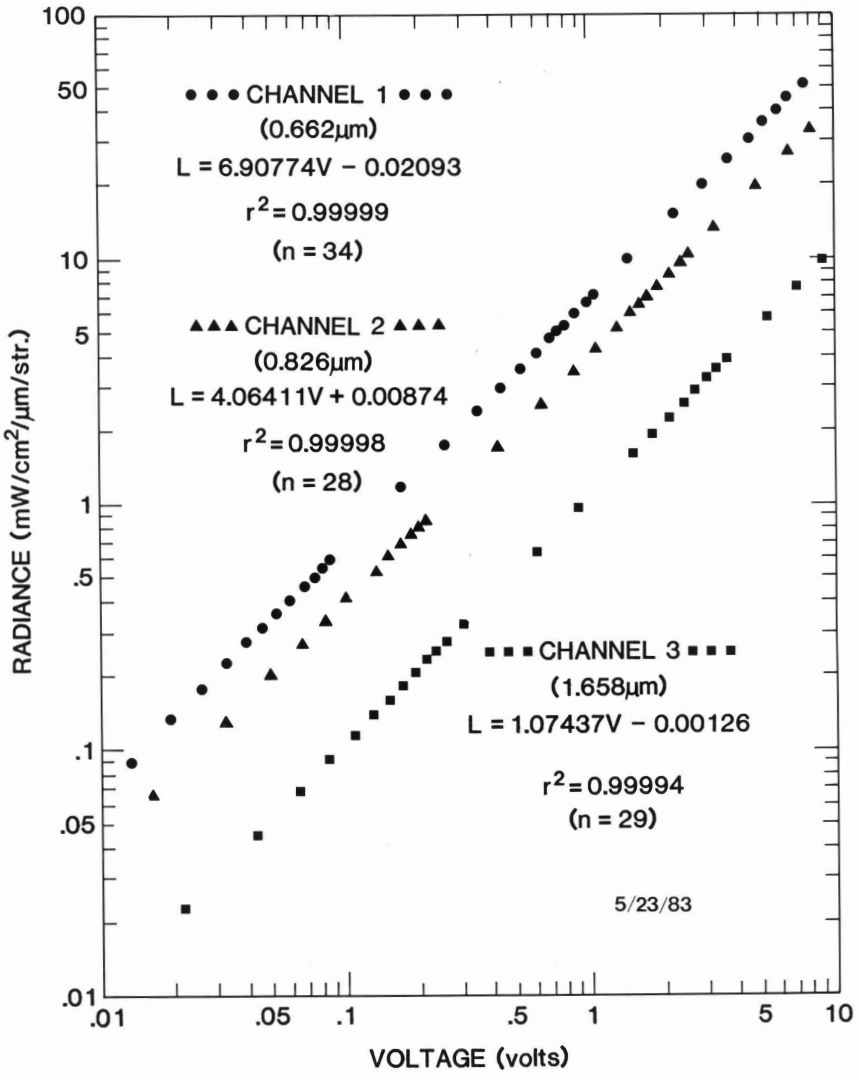

Figure 7. Integrating sphere radiance relationships to PARABOLA sensor Channels 1, 2 and 3 measured voltage outputs.

PARABOLA DATA PRESENTATION

The radiometric data acquired for each PARABOLA IFOV as the instrument scans the sky and ground targets represent a variety of spatially distributed shapes, such as circles, ellipses, parabolas or hyperbolas, depending on the view angle. For ground targets the IFOV "footprints" are typically circular at the nadir position and become increasingly larger ellipses as the off-nadir angle increases (Figure 8). If the off-nadir view angle η is less than $\pi/2-\alpha$ (where

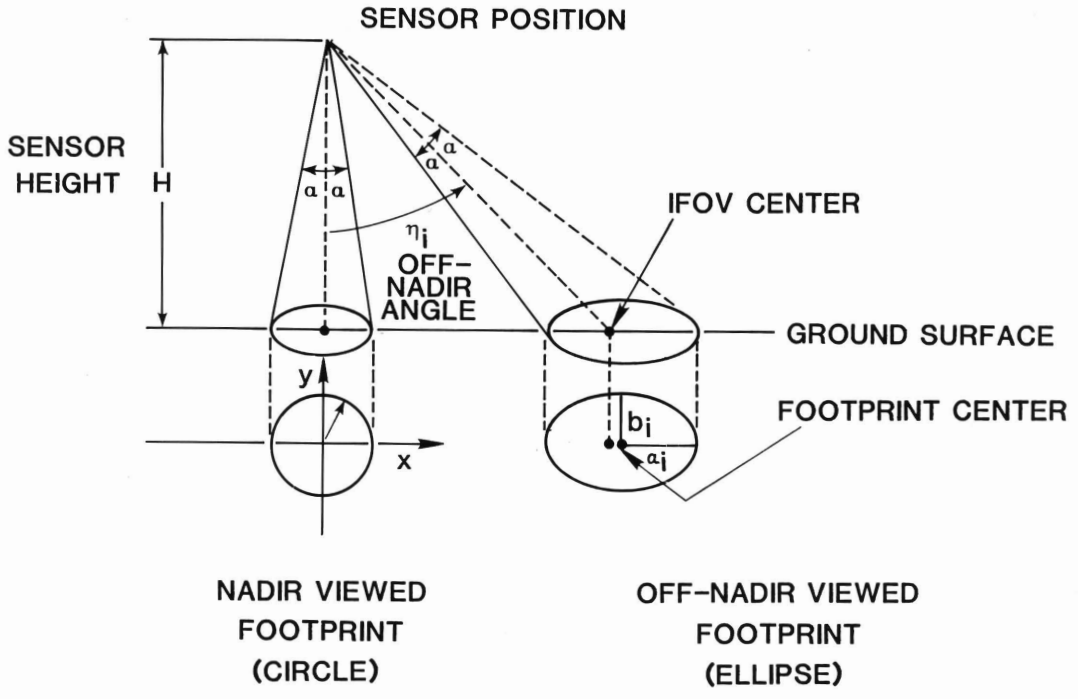

Figure 8. Footprints of a PARABOLA sensor IFOV on the Ground.

α=1/2 the IFOV angle), it will be an ellipse whose major and minor axes are given by

$$a_i = \frac{H \tan\alpha \, (1 + \tan^2\eta_i)}{1 - (\tan\alpha \tan\eta_i)^2}$$

$$b_i = \frac{H \tan\alpha}{\cos\eta i \left[1 - (\tan\alpha \tan\eta_i)^2\right]^{1/2}}$$

where

H = sensor height

$$\eta_i < \frac{\pi}{2} - \alpha$$

Then, the area of the elliptic footprint can be computed by

$$A_i = \pi a_i b_i$$

Thus, for a sensor height of 6 m the nadir circular footprint with a radius of 0.79 m (at 15° IFOV) has a surface area of 1.96 m^2 from $(H\tan\alpha)$, while the 45° and 60° off-nadir angles with ellipse major axes (a) of 1.61 m and 3.37 m, respectively, measure surface areas of 5.7 m^2 and 17.3 m^2, respectively. Therefore, the interpretation of off-nadir angular measurements from PARABOLA or any other sensor requires careful documentation and understanding of the scene elements contained within each pixel. Due to the helical scan pattern and the non-sampled 15° region at the view angles toward the sensor mount device, the resulting pattern of IFOV ground footprints is as presented in Figure 9 for off-nadir angles to 75°. Beyond 75° off-nadir (IFOV center) the IFOV pixel will usually include both sky and ground radiance contributions. The PARABOLA sensor cones that measure sky radiance do not intersect a natural plane (unless it is a cloud layer) as do the downward viewing sensor cones; thus a projection was chosen as presented in Figure 9 to represent the sky data spatially on a two-dimensional surface (see also Appendix B).

The actual sensor positions, as defined in measured "elevation" and roll angles, are converted to the off-nadir angles and azimuths

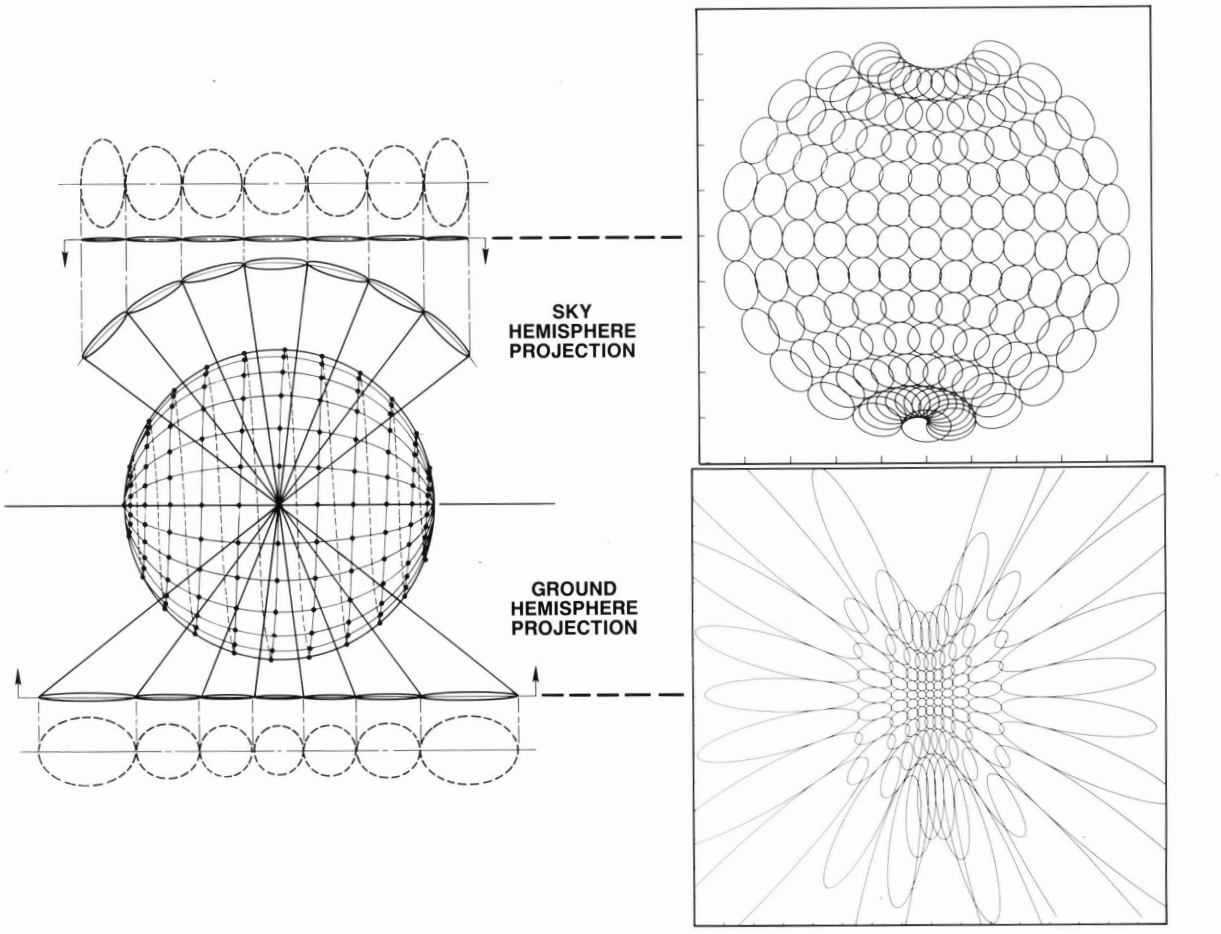

Figure 9. Representative projections of PARABOLA IFOV pixels onto two-dimensional surfaces as used for data interpretations.

individually for each scan data set through special software developed for the PARABOLA (Park and Ostroff, 1983; Appendix C). PARABOLA data are normally presented as computed radiances on the actual sky or ground pixel prints, as grey-tone or color radiance images, or as tabular listings by sequential pixel number and viewing angle for further processing and analysis. A typical data processing sequence is presented in Figure 10.

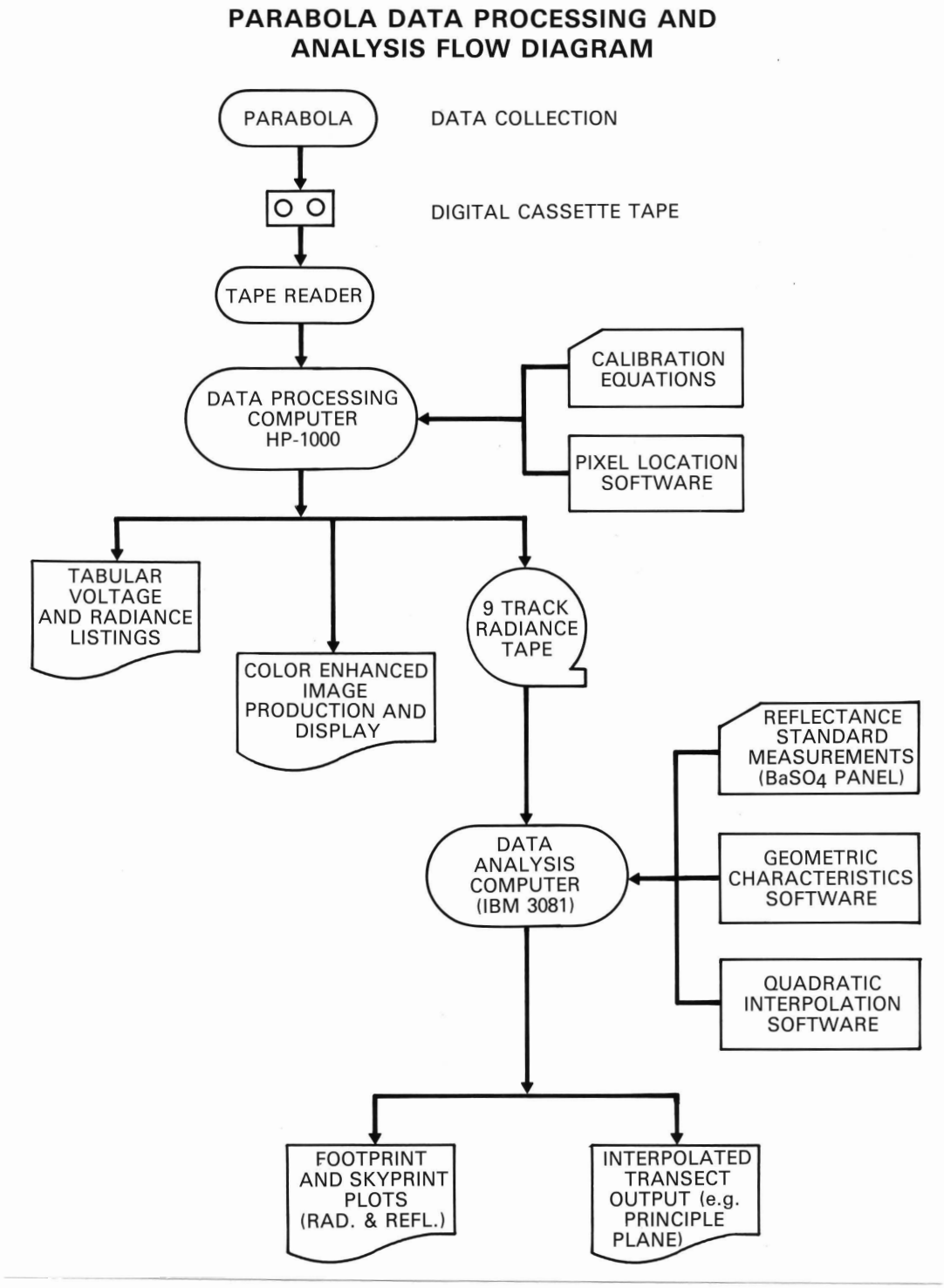

Figure 10. PARABOLA data processing and analysis flow chart.

PARABOLA PLATFORM SYSTEMS

The first device built to support the PARABOLA sensor head for laboratory and field data collection was a heavy-duty tripod-and-boom mount (Figure 11) capable of taking measurements from a maximum height of 2 to 2.5 m above the ground target. The support boom consists of a pole with a sensor head locking collar mount with a counter-balance weight and electrical connector on the opposite end. Located close to the sensor head on the pole is a horizontal sensor head level indicator in the form of a precision electronic pendulum, which has a direct digital readout on the control panel. The "roll"

Figure 11. PARABOLA tripod mount apparatus in use on a bare soil site.

is controlled by a bubble level on the tripod and an alignment mark on the pole. Aside from necessary laboratory testing and calibration uses of the tripod mount, other applications include bidirectional measurements of bare soil surfaces and relatively homogeneous, short and closely spaced grass and broadleaf plant covers, forest within-canopy radiant energy penetration and distribution measurements, measurement of certain man-made surfaces, and sky radiance distribution measurements.

Another PARABOLA sensor head mount was developed for use on the large Goddard boom-equipped instrument van, which required the construction of hardware to attach the sensor head to the gimbaled and motorized boom head and a long (15 m) electronics cable (Figure 12). A downward looking camera mount was also added. This same basic sensor head support apparatus was used with an additional specialized bracket to mount the instrument to the gondola of a hot air balloon (Figure 13). Both the instrument van and balloon platforms have been successfully used to acquire field data.

The van is particularly well suited to controlled plot (e.g., agricultural field) experiments and can elevate the sensor to almost 10 meters above the ground, although normal operating height is 5-7 meters to maximize the horizontal extension of the sensor away from the vehicle. The primary disadvantages of the van are related to the size of the vehicle. The van with its instrument boom assembly is 6.7 m (22 ft.) long and 2.1 m (7 ft.) wide and weighs 5,440 kg (12,000 lbs.). The weight restricts its use to good "road" conditions (e.g., firm, dry), which can cause missed measurement opportunities that may be critical to an experiment. In addition, the maneuverability

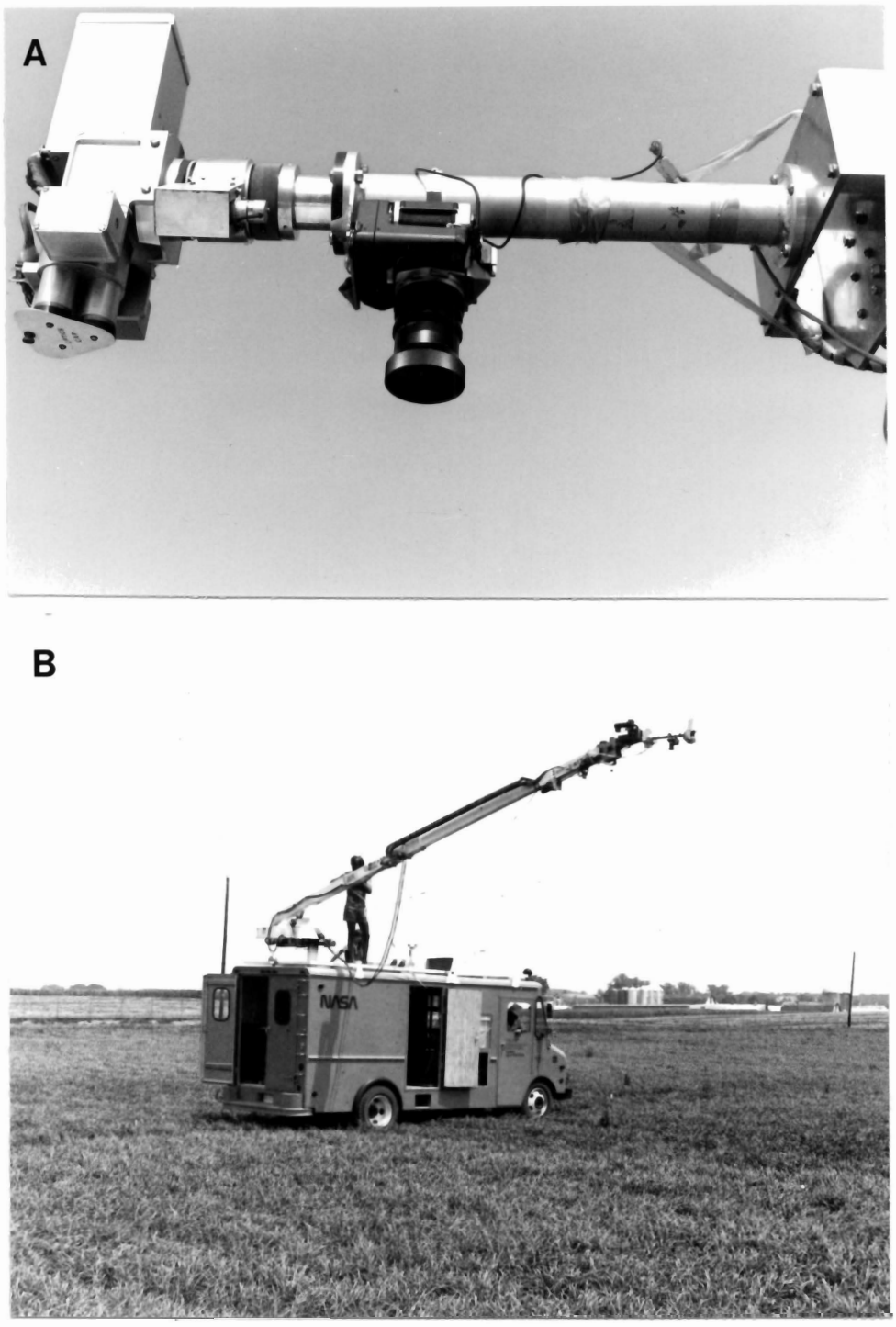

Figure 12. Instrument van boom with PARABOLA sensor and camera (A) and van in operation (B).

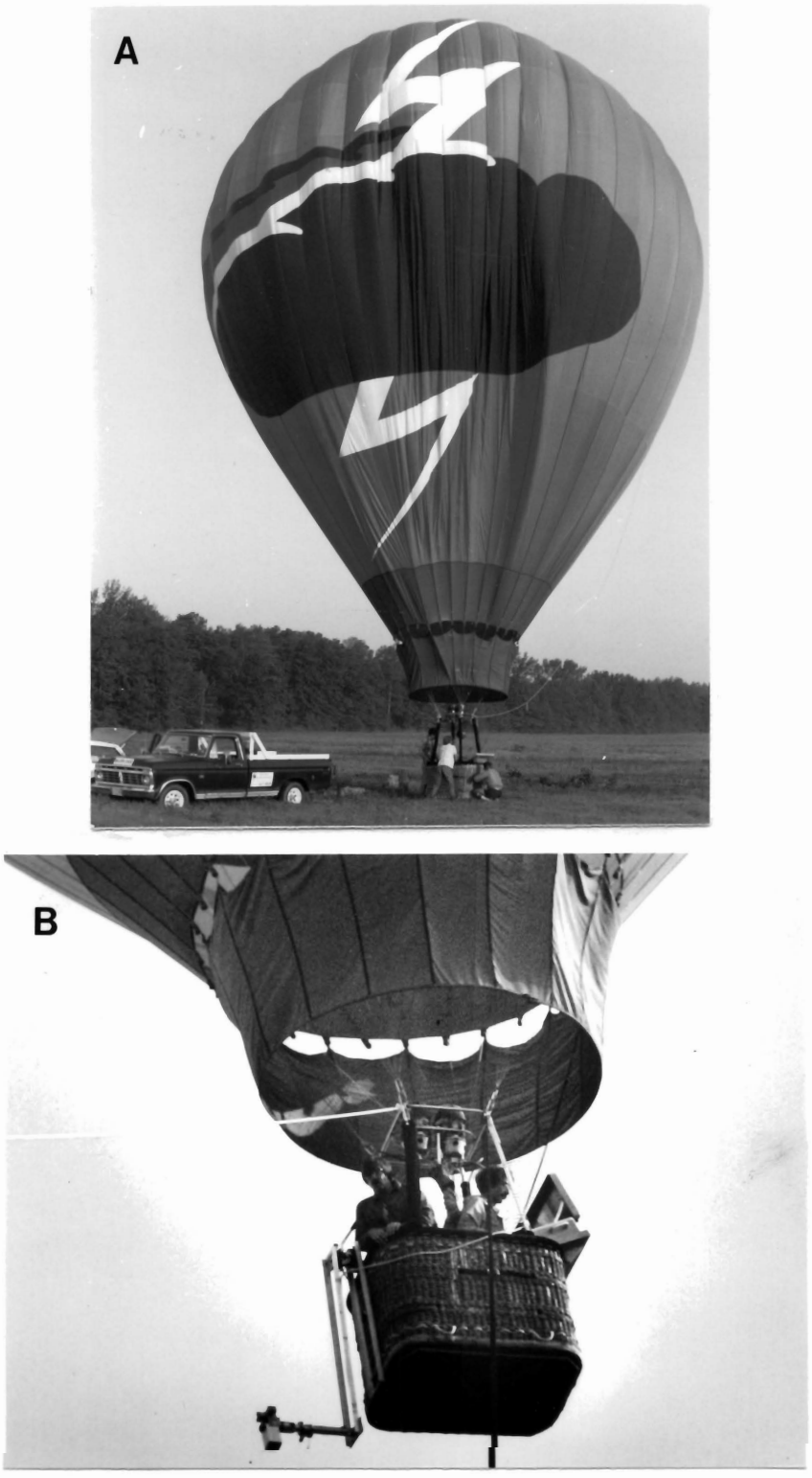

Figure 13. Hot air balloon (A) and gondola with PARABOLA sensor suspended below gondola (B). Data system box is mounted on gondola basket hand rail.

is not good for quickly relocating from site to site. This is especially true when sharp turns are required and accurate boom alignment is necessary for an experiment; for example, to maintain sensor axis orientation relative to the constantly changing solar azimuth.

The hot-air balloon mount provides the necessary height capability and a stable platform for forest canopy measurements. Helicopter mounting consideration was initially rejected because of concern over potentially damaging vibrations and sensor leveling stability, as well as the attendant costs that would have been required for such protection and helicopter integration. Drawbacks of the balloon use primarily result from the meteorological limitations of low windspeed and thermal activity for safe flight and the lack of speed and directional controls for specific site sampling. However, with a good pilot and proper conditions successful measurement sampling can be conducted. One additional benefit of the balloon operation, as compared with the other platforms used, is that the support platform does not block the ground target at any viewing angle. However, the associated drawback is that the sky irradiance distribution measurements are signficantly obstructed, as is apparent from Figure 13.

Transportable Pickup Mount System

The PARABOLA sensor was primarily designed to be a field instrument. Based on the requisite experience from two growing seasons of data collection with the instrument van and tripod platforms, a new sensor platform was designed that would preserve and enhance the portability feature originally designed into the basic PARABOLA instrument system. The Transportable Pickup Mount System or TPMS (Figure 14) is basically

Figure 14. PARABOLA sensor in use with the Transportable Pickup Mount System on a four-wheel drive pickup in a sand shinnery oak rangeland plant community.

a light-weight, collapsible boom apparatus that is easily transported via commerical airline or other public conveyance for simple adaptation and mounting on any standardsized pickup truck (e.g., U.S.A. makes or similar bed designs).

The primary support beam is an aluminum triangular truss, 18 cm on a side, that decouples as four, 2 m long sections. A secondary support beam is a two-piece telescoping rod (each piece approximately 1.5 m long and 4 cm square) that supports a cable wind-up winch at its base. At the top end of the primary beam rests a detachable, two-axis motorized PARABOLA sensor mounting/leveling/camera head (Figure 15). The remaining hardware consists primarily of 1) two

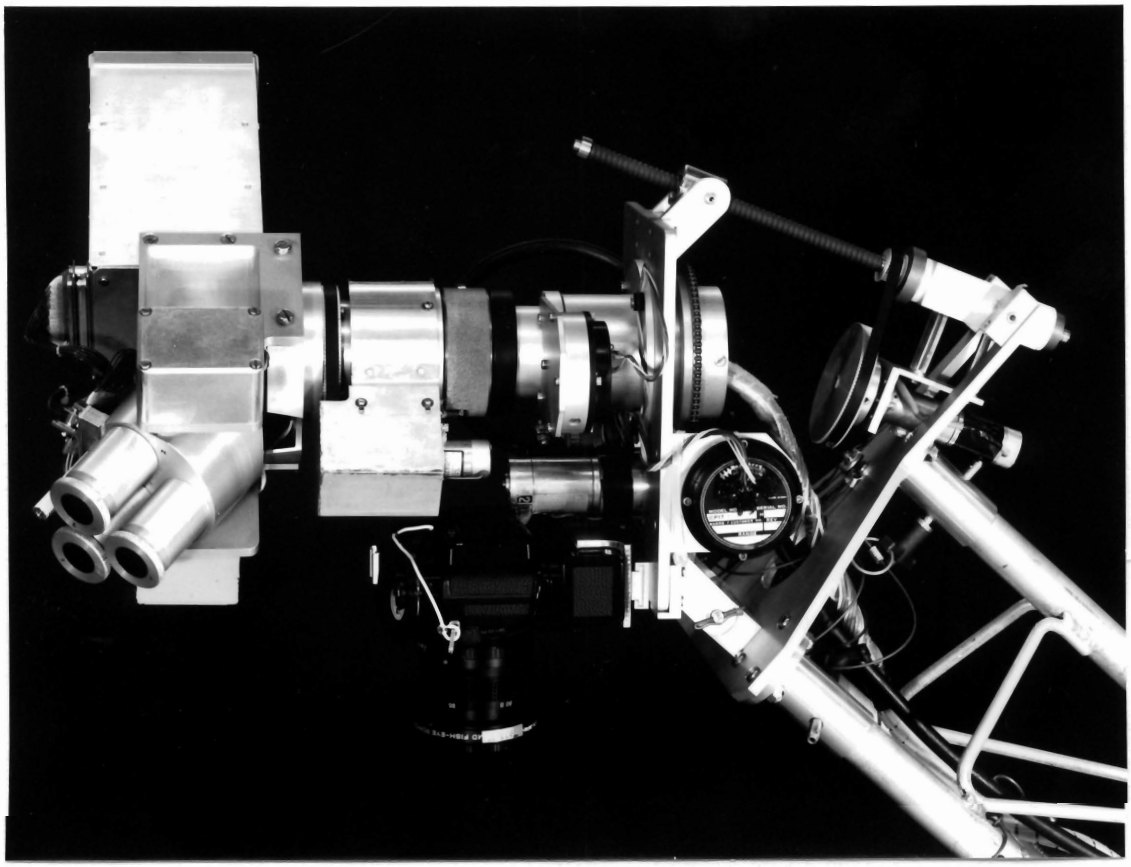

Figure 15. Motorized TPMS head on primary support beam with PARABOLA sensor and automatic motorized fisheye camera in operating configuration.

specially engineered pickup bed post hole, swivel anchor mounts that support the primary and secondary beams, 2) four pickup bed corner post hole anchors, 3) various lengths of 3 mm diameter twisted steel cabling with length-adjustable turnbuckles, and 4) an electronics cable that connects the leveling head to the PARABOLA data system (Figure 1).

The primary support beam has been designed to hinge at its mid-point so that the head can be easily lowered, via the winch and primary cable, to any height down to near ground level while the lower half-section remains stationary. This feature enables reflectance standard, calibration, and direct solar beam (neutral density filtered) measurements to be taken and film to be changed in the camera without dismantling the boom apparatus. Additionally, with the pickup bed swivel mounts at the base of the primary beam, the boom can be folded in half rotated 90°, and stored over the cab of the pickup for traveling relatively short distances between study sites without being dismantled.

All operations of the PARABOLA/TPMS, except for raising and lowering the boom, are controlled from the PARABOLA data system control panel. These include normal sensor operations as well as sensor head leveling (pitch and roll) and remote camera triggering and counting. In addition to ground target photo documentation with the downward looking automatic exposure camera equipped with a 16 mm fisheye lens and motor drive, normal data acquisition procedure includes documenting the complete sky condition with an upward looking camera equipped with a 7.5 mm fisheye lens. Both cameras have LED imprinters that record the exact time of exposure directly on each photo to enable accurate comparison with the PARABOLA radiometric data.

The primary boom support cable that is used for raising and lowering the boom and sensor head is attached to a worm-gear-driven winch with a 40:1 drive ratio. This high ratio was chosen to provide a safety factor to prevent accidental release of trip-lock mechanisms that might have been used. However, this makes hand-cranking the cable a rather laborious task. Thus, to make the cranking task faster and less tedious for normal operations a small 12 volt D.C. to 115 volt A.C. power inverter is connected to the pickup battery to provide up to 400 watts of electric power to drive a 4.5 ampere, 10 mm (3/8 inch) bit variable speed reversing drill. A special "drill bit" adapter was engineered to mate with the winch crank gear drive. At 1200 rpm drill speed the boom can be quickly raised and lowered.

The complete PARABOLA/TPMS hardware assemblage is carried in only four hand-carrying cases (Figure 16), excluding cameras. A large triangular shaped canvas bag provides foam pad protection to the aluminum support beams and when loaded weighs approximately 30 kg (65 lbs.). A small square, padded wooden case protects the PARABOLA sensor head and with the head weighs a total of 9 kg (20 lbs.). The remaining two suitcase-sized fiberglass boxes contain the PARABOLA data system and the miscellaneous hardware, steel and electrical cables, and TPMS mounting head. Each of these boxes weighs approximately 30 kg (65 lbs.).

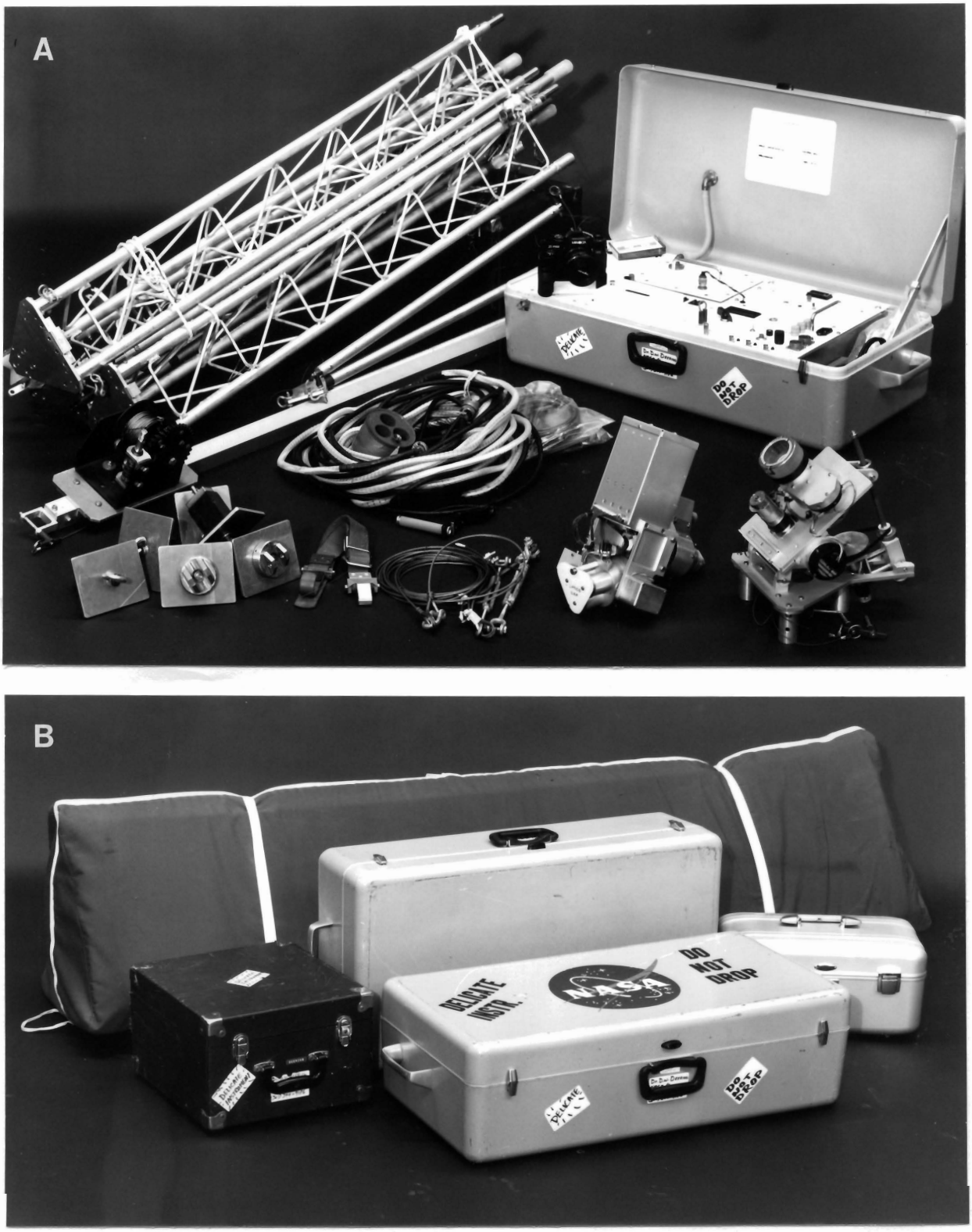

Figure 16. PARABOLA/TPMS component hardware disassembled for storage (A) and in carrying case (B).

CONCLUSIONS

The measurements made with this instrument will improve our understanding of the bidirectional reflectance properties of natural earth surface covers under a variety of illumination conditions. Through empirical modeling and testing of theoretical surface cover models, measurements such as those obtainable with the PARABOLA should eventually enable the accurate computation of earth surface and planetary albedos using satellite data and make possible corrections to reflectance measurements of earth features, whether measured from a nadir-looking or an off-nadir pointing sensor, and including such sensors as the wide angle viewing AVHRR. This capability and understanding will lead to improved assessments of earth surface features and vegetation attributes from spaceborne sensors using off-nadir, multiple angle measurements, such as the French SPOT system and other future pointable sensors as may be flown on the space shuttle or EOS Space Station platforms.

It has been the purpose of this paper to inform the remote sensing community of the characteristics and capabilities of the rather unique PARABOLA remote sensing field instrument and the attendant sensor platforms that have been developed to enable the collection of multidirectional radiance data for a wide variety of vegetation types and the incident sky irradiance field. Although this instrument is a prototypical one-of-a-kind, and therefore not available for purchase in the marketplace, it is hoped that this paper will both foster and guide future development of similar, improved instruments as well as stimulate the thinking of other scientists and engineers.

ACKNOWLEDGEMENTS

The authors wish to thank GSFC engineers (Code 674) Max Strange, Fred Blaine, and Frank Russo for their contributions to the electronic, optical and data system designs of the PARABOLA instrument and to Ken Kirks for his assistance in building the TPMS. Acknowledgement is also due to John Park (SAR contractor) and Bob Sullivan (GSFC Code 673) for their efforts in developing the data processing and analysis software. Special thanks go to Tom Eck (SAR contractor) and Frank Wood (GSFC Code 623) who have been so valuable in the field measurements, instrument testing and data processing/analysis facets of the PARABOLA capability evolution and to Charles Schnetzler (GSFC Code 622) who gave primordial impetus to the PARABOLA development.

REFERENCES

Barnsley, M.J. (1984), Effects of off-nadir view angles on the detected spectral response of vegetation canopies. Int. J. Remote Sensing, 5, 715.

Colwell, J.E. (1974), Grass canopy bidirectional spectral reflectance. In Proceedings, Ninth Int. Symp. on Remote Sensing of Environment, Univ. Michigan, Ann Arbor, pp. 1061-1085.

Eaton, F.D. and Dirmhirm, I. (1979), Reflected irradiance indicatrices of natural surfaces and their effect on albedo. Appl. Optics, 18, 994.

Egbert, D.D. and Ulaby, F.T. (1972), Effects of angles on reflectivity. Photogramm. Engng. Remote Sensing, 38, 556.

Goel, N.S., Strebel, D.E. and Thompson, R.L. (1984), Inversion of vegetation canopy reflectance models for estimating agronomic variables. II. Use of angle transforms and error analysis as illustrated by Suits' model. Remote Sensing Environ., 14, 77.

Hughes, N.A. and Henderson-Sellers (1982), System albedo as sensed by satellites: its definitions and variability. Int. J. Remote Sensing, 3,1.

Kimes, D.S. (1983), Dynamics of directional reflectance factor distributions for vegetation canopies. Appl. Optics, 22, 1364.

King, M.D. and Curran, R.J. (1980), The effect of a non-uniform planetary albedo on the interpretation of earth radiation budget observations. J. Atmos. Sci., 37, 1262-1278.

Kirchner, J.A., Kimes, D.E., and McMurtrey III, J.E. (1982), Variation of directional reflectance factors with structural changes of a developing alfalfa canopy. Appl. Optics, 21, 3766.

Kriebel, K.T. (1976), On the variability of the reflected radiation field due to differing distributions of the irradiation. Remote Sensing Environ., 4, 257.

Kriebel, K.T. (1978), Measured spectral bidirectional reflection properties of four vegetated surfaces. Appl. Optics, 17, 253.

Ott, W., Pfeiffer, B. and Quiel, F. (1984), Directional reflectance properties determined by analysis of airborne multispectral scanner data and atmospheric correction. Remote Sensing Environ., 16, 47.

Park, J.K. and Deering, D.W. (1984), Biomass/soil-reflectance relationships for changing sensor view angles and sun elevations. Appl. Optics (submitted).

Park, J.K. and Ostroff, T. (1983), PARABOLA instrument geometric characteristics software user's guide. Systems and Applied Sciences Corporation report to NASA/GSFC. 28 p. (unpublished).

Ranson, K.J., Vanderbilt, V.C., Biehl, L.L., Robinson, B.F. and Bauer, M.E. (1981), Soybean canopy reflectance as a function of view and illumination geometry. In Proceedings, Fifteenth Int'l. Symp. on Remote Sensing of Environ., Univ. Mich., Ann Arbor, pp. 853-865.

Rao, V.R., Brach, E.J. and Mack, A.R. (1979), Bidirectional reflectance of crops and the soil contributions. Remote Sensing Environ., 8, 115.

Salomonson, V.V. (1966), Anisotropy of reflected solar radiation from various surfaces as measured with an aircraft-mounted radiometer. In Proceedings, Fourth Symp. on Remote Sensing of Environ., Univ. Mich., Ann Arbor, pp. 393.

Salomonson, V.V. and Marlatt, W.E. (1968), Anisotropic solar reflectance over white sand, snow and stratus clouds. J. Appl. Meteorol., 7, 475.

Salomonson, V.V. and Marlatt, W.E. (1971), Airborne measurements of reflected solar radiation. Remote Sensing Environ., 2, 1.

Smith, J.A. (1980), Scene radiation and atmospheric effects characterization basic research planning effort. Final Report (NAS 9-16016) NASA/ Johnson Space Center, August 1980, 80 pp.

Smith, J.A. and Oliver, R.E. (1974), Effects of changing canopy directional reflectance on feature selection. Appl. Optics, 13, 1599.

Steven, M.D. (1977), Standard distributions of clear sky radiance. Quart. J. Roy. Meterol. Society, 103, 457.

Vanderbilt, V.C., Grant, L., Biehl, L.L. and Robinson, B.F. (1983), Specular, diffuse and polarized light scattered by two wheat canopies. Appl. Optics (submitted).

Verhoef, W. and Bunnik, N.N.J. (1976), The spectral directional reflectance of row crops. Part 1: Consequences of non-Lambertian behavior for automatic classification. Part 2: Measurements on wheat and simulations by means of a reflectance model for row crops. Tech. Report No. NIWARSPUBL-35, Netherlands Interdepartmental Working Group on the application of Remote Sensing, Delft.

APPENDIX A

PARABOLA INSTRUMENT FUNCTIONAL DIAGRAM

The PARABOLA instrument components, consisting primarily of the scan head system and data system, have been generally described in the main body of this report. The functional interrelationships between these components as they operate through the various key elements within each component have not been detailed. Therefore, Figure A-1 is presented here in order to help clarify these interrelationships.

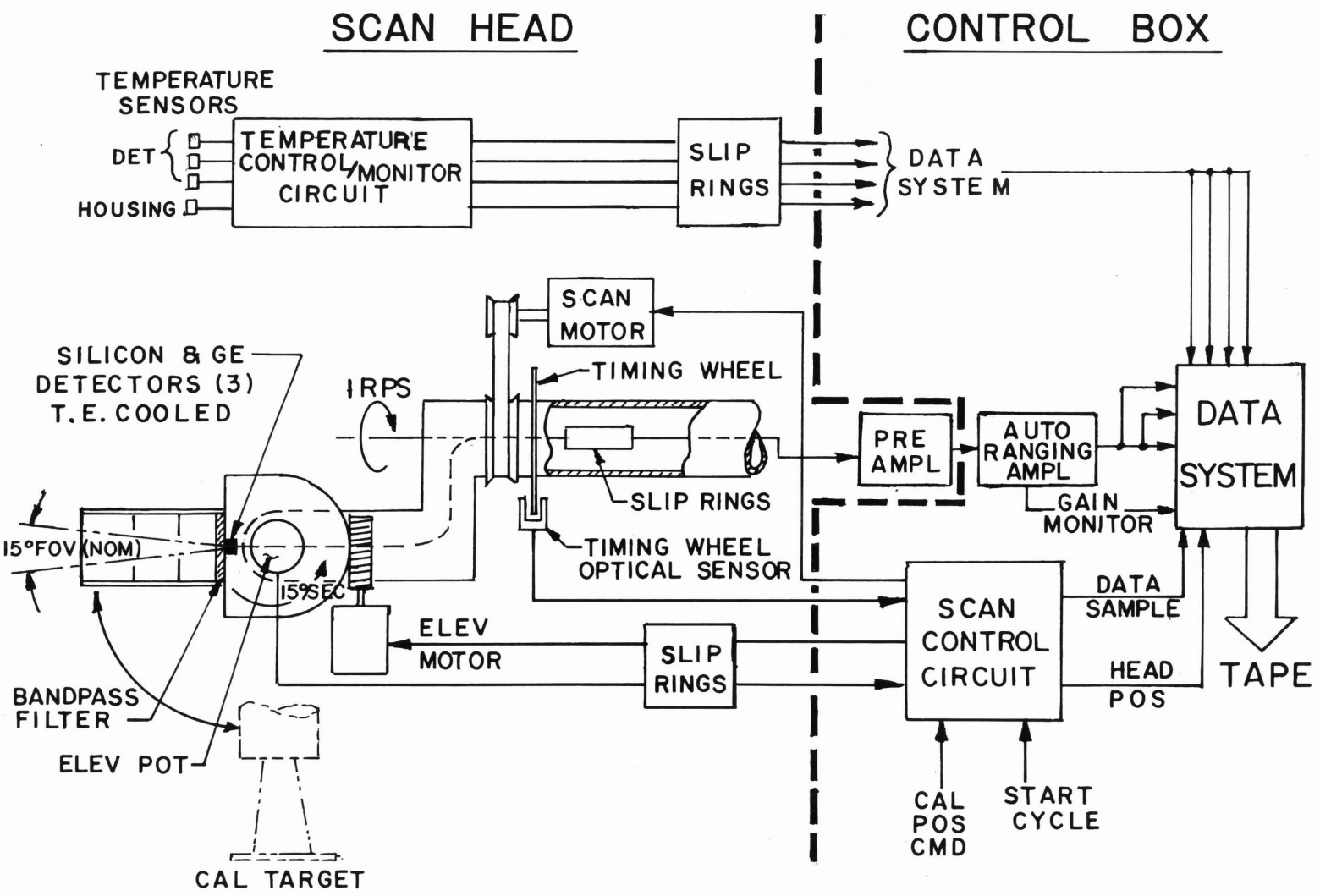

Figure A-1. PARABOLA instrument functional diagram.

APPENDIX B

PARABOLA DATA PRESENTATION AND MEASUREMENT EXAMPLES

Because the geometric characteristics of the PARABOLA radiometric measurements are somewhat complicated, especially as they relate to the interpretation and presentation of the data, Figures B-1 through B-2 are given to help clarify these geometric features. The sky hemisphere is depicted in Figure B-1 and the ground hemisphere is shown in Figure B-2.

The routine data outputs for PARABOLA measurement data are illustrated in the partial tabular computer printout listings of 1) "raw" voltage data (Figure B-3) used primarily in engineering tests and 2) computed radiance data (Figure B-4) that incorporate radiometric calibration data and provide an easily readable format. A next frequently used procedure for understanding the radiance distribution characteristics of a field measurements data set is to produce a spatial "pixel print" upon which the radiance data are superimposed, as illustrated in Figure B-5.

It is generally recognized that the predominant features of a target's bidirectional reflectance distribution function are found along the solar principal plane. Thus, a procedure has been developed to compute the solar principal plane (or any other azimuth transect) radiance values for the ground target from the spatial matrix of PARABOLA pixels. This procedure and a couple of examples are given in Figure B-6.

Three other techniques for representing the sky and ground radiance distributions are given in Figures 7 through 10 and include insoline contouring, grey-tone pixel "mapping" and an interpolated high resolution matrix wherein radiance (or computed reflectance) levels are color coded.

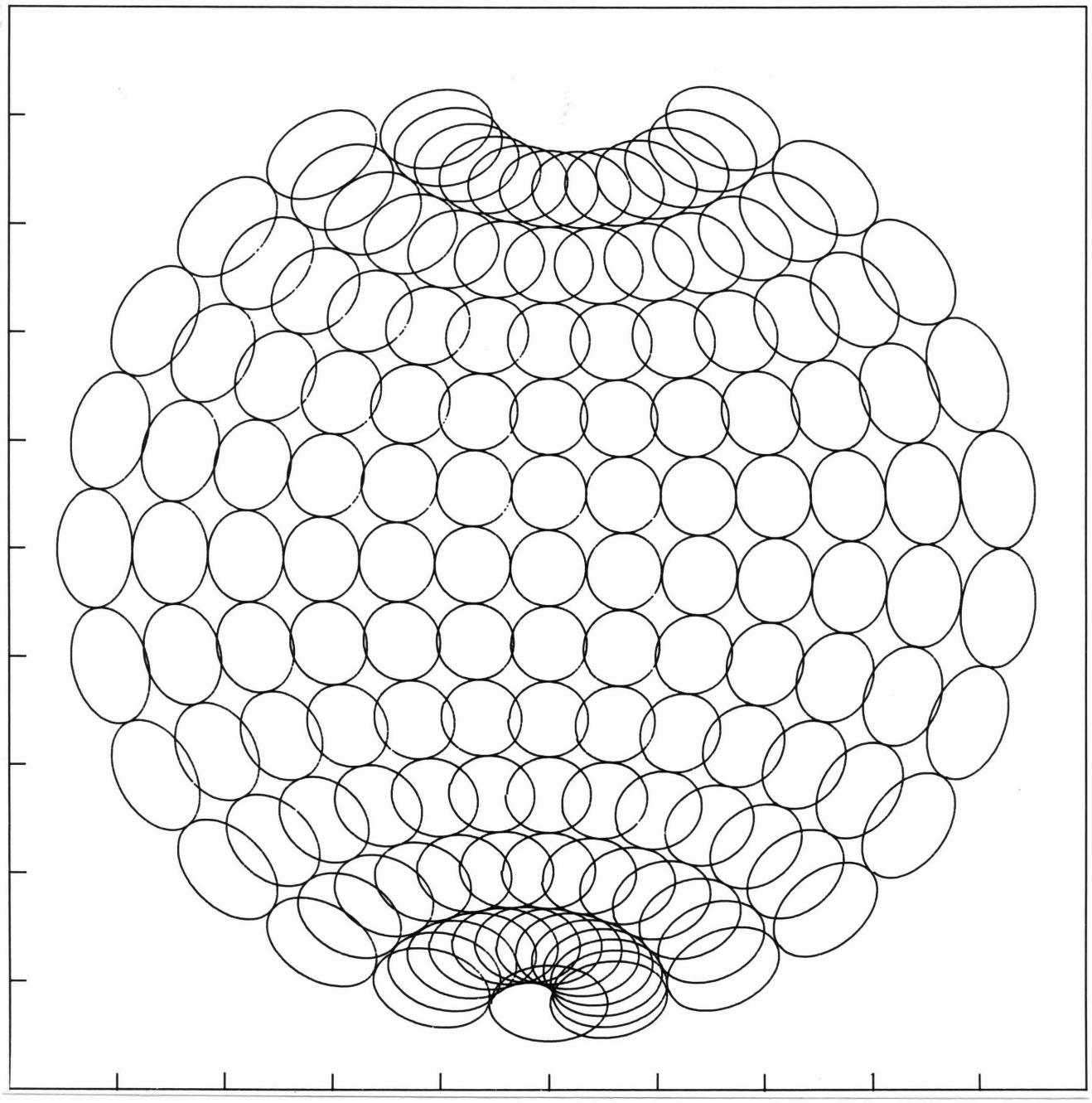

Figure B-1a. Sky hemisphere IFOV pixel print; a typical sampling scan pattern.

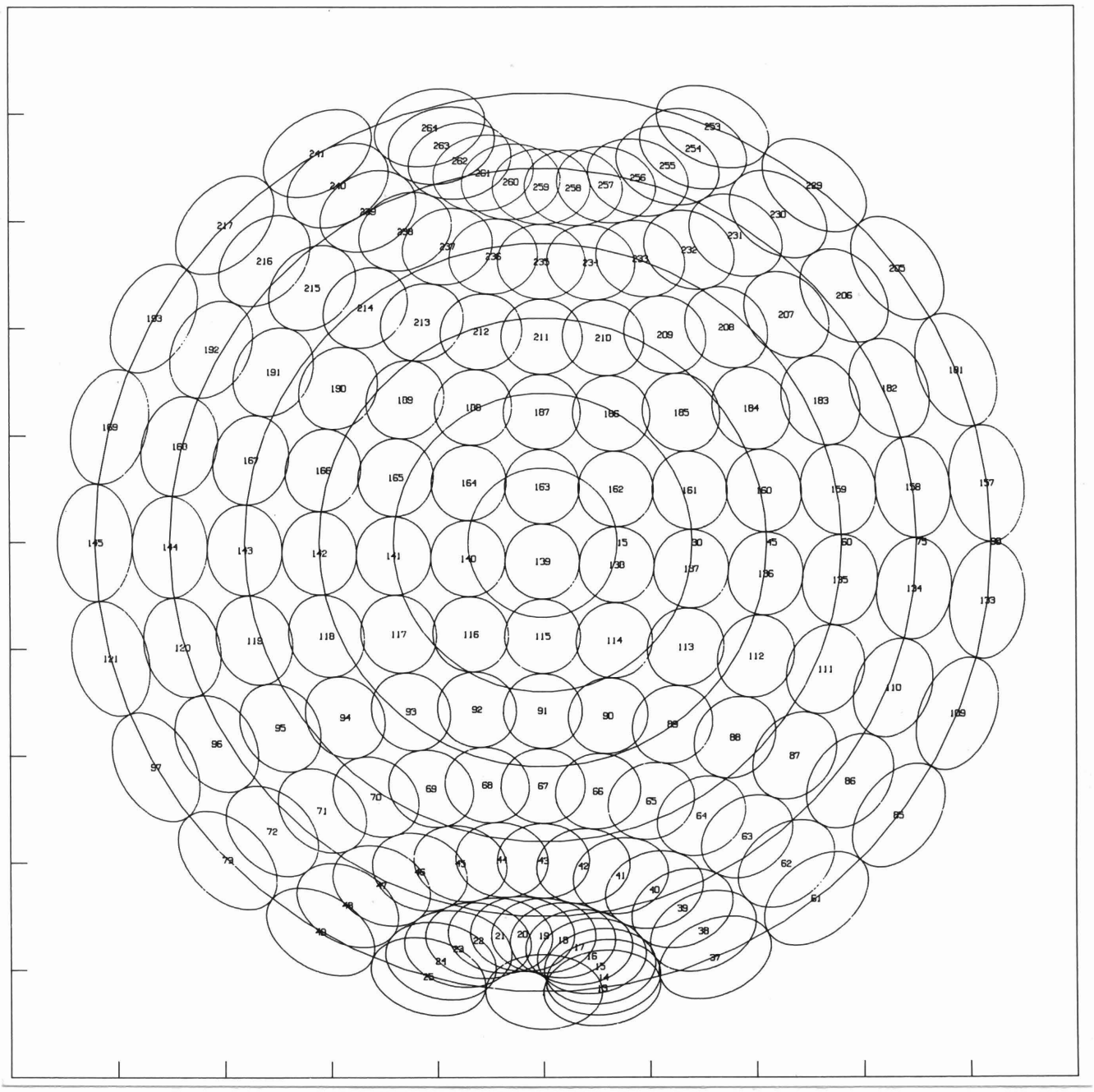

Figure B-1b. Sky hemisphere IFOV pixel print showing representative scan sequence pixel accession numbers, with a 15° increment concentric pattern of off-nadir view angles superimposed.

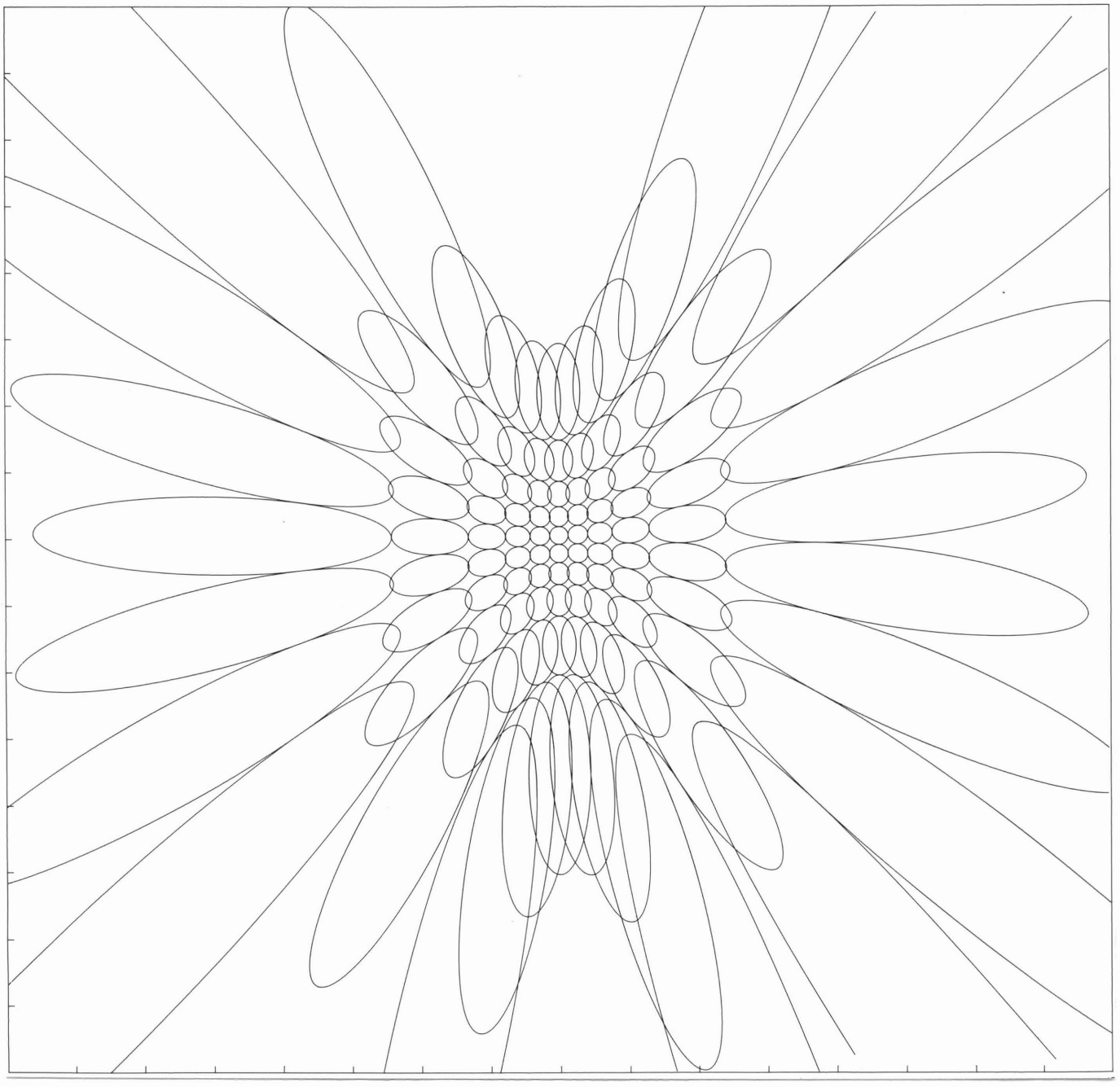

Figure B-2a. Ground hemisphere IFOV pixel print ("footprint"), a typical sampling scan pattern.

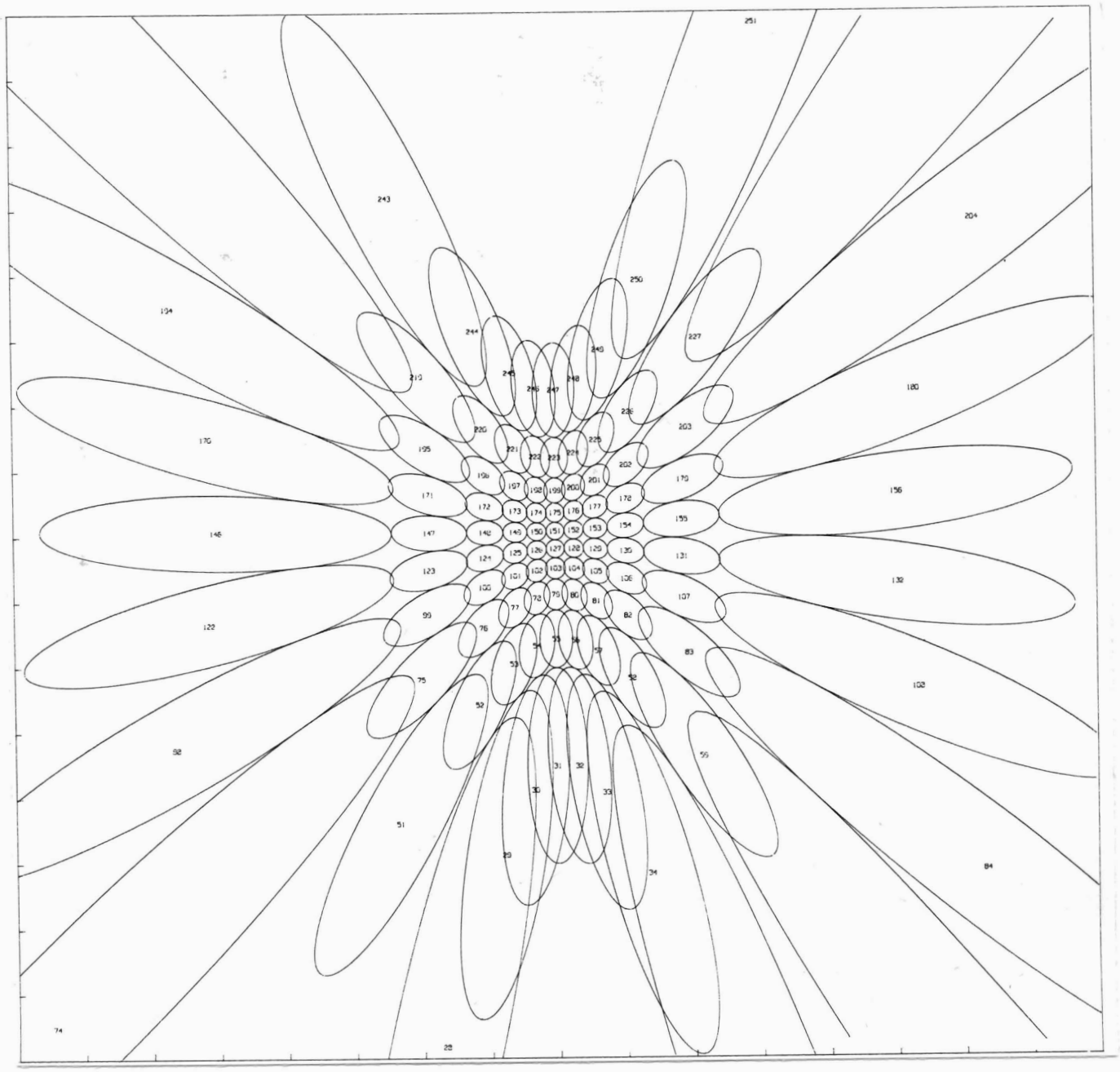

Figure B-2b. Ground hemisphere pixel footprint showing representative scan sequence pixel accession numbers.

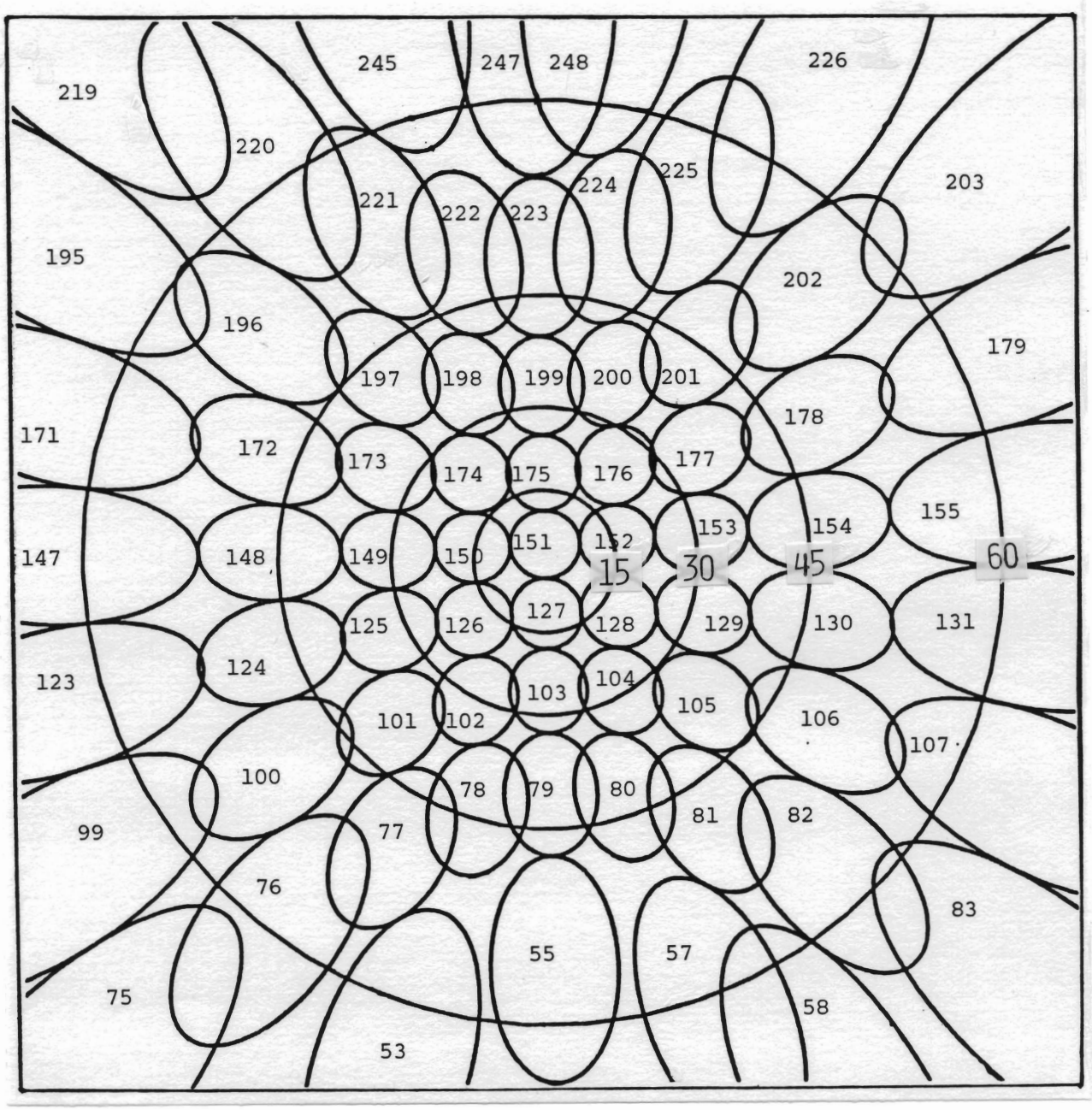

Figure B-2c. An enlarged ground pixel footprint showing representative pixels for up to approximately 60° off-nadir view angle (subset used in analysis).

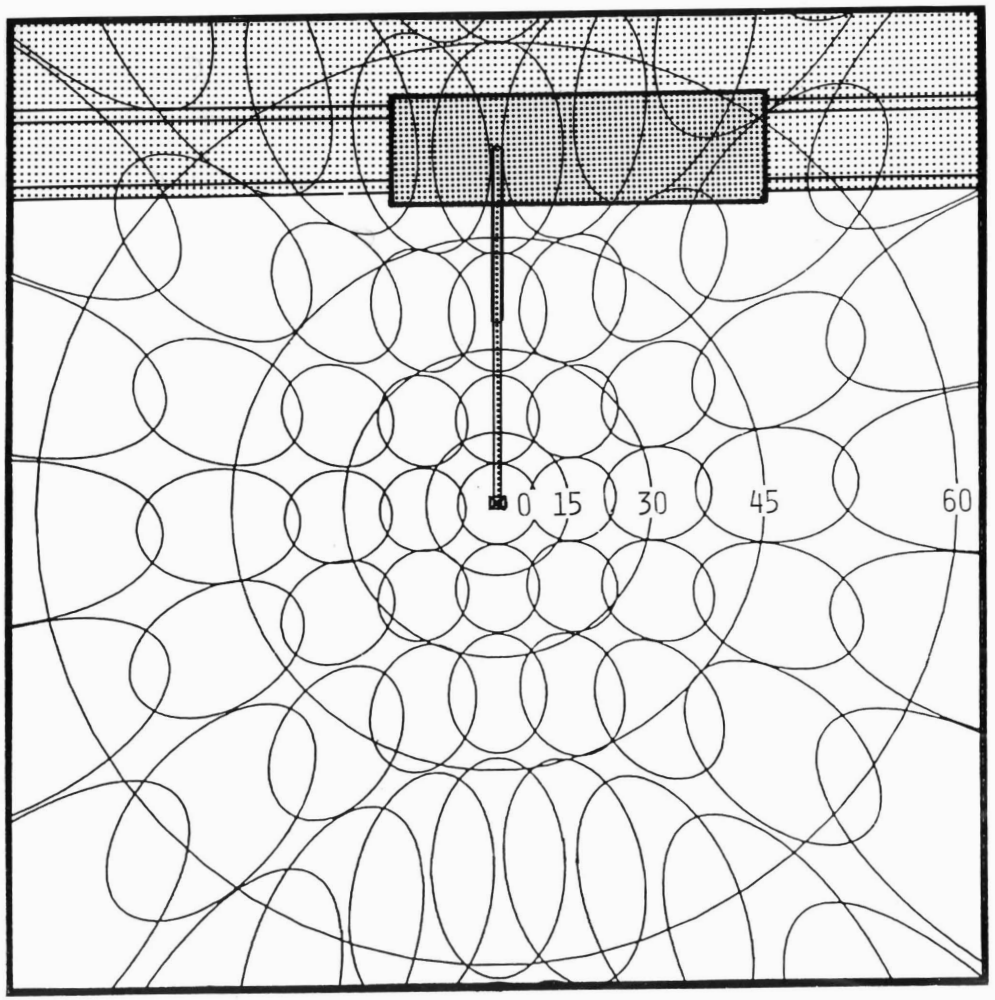

- PARABOLA AT 5 METERS ABOVE TARGET SURFACE.
- CONCENTRIC RINGS SHOW OFF-NADIR VIEWING ANGLE INTERVALS OF 15°
- FOV'S SHOWN ARE AT 17° (98% RESPONSE LEVEL)

Figure B-2d. PARABOLA footprint relationship to support platform van.

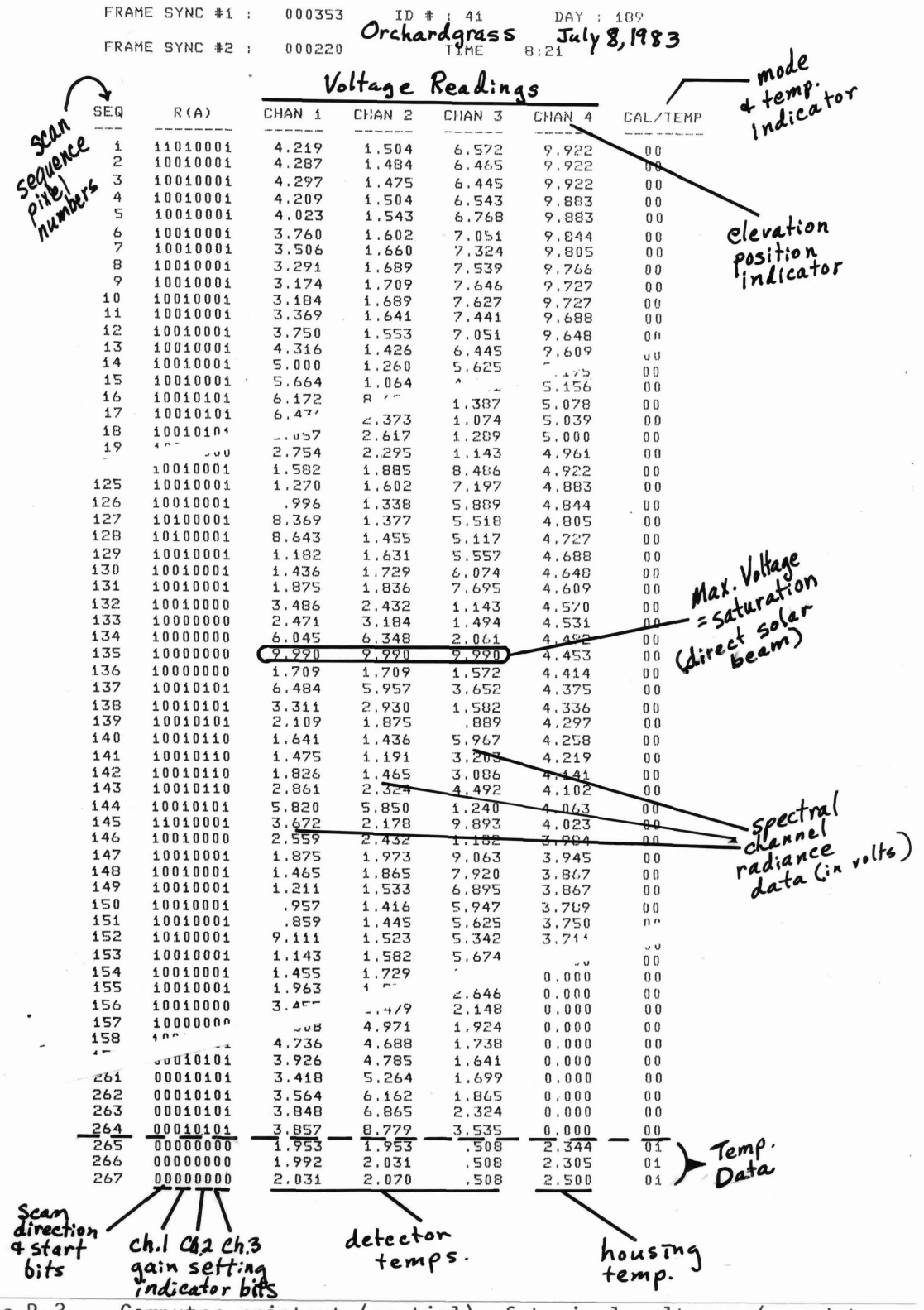

Figure B-3. Computer printout (partial) of typical voltages (raw data output) from a PARABOLA scan showing certain key features of the data stream.

********** TAPE ID = 83-0

INSTRUMENT IN DATA COLLECTION MODE.

Orchardgrass (c-cut) Plot

ID # : 13 DAY : 225 TIME 9:02 DATE : 08-10-83

PIXEL NO.	HEMI-SPHERE	VIEW AZ (DEG)	NADIR ANGLE (DEG)	RADIANCES(MW/CM.SQ.) CHAN #1	CHAN #2	CHAN #3	ELEV (DEG)
1	L	178.71	90.00	3.35	5.60	.86	1.29
2	L	178.75	89.67	3.37	5.53	[illegible]	
3	L	178.88	89.36	[illegible]			
4	L	[illegible]			[illegible]	1.54	83.14
				5.01	7.39	1.68	83.79
	L	97.85	45.27	2.50	6.04	1.48	84.43
125	L	98.51	30.28	2.07	5.01	1.24	85.72
126	L	103.78	15.42	1.56	4.45	1.00	86.37
127	L	180.00	2.99	1.48	3.87	.90	87.01
128	L	261.01	15.18	1.31	3.76	.85	87.66
129	L	266.60	30.04	1.15	3.96	.86	88.30
130	L	268.51	45.01	1.20	4.18	.89	88.95
131	L	269.53	60.00	1.44	5.13	1.06	89.59
132	L	270.24	75.00	1.45	7.03	1.43	90.23
133	L	270.88	90.00	16.03	10.53	1.68	90.88
134	U	271.58	104.99	36.47	18.23	2.19	91.52
135	U	272.50	119.98	68.99	40.61	10.73	92.17
136	U	274.88	134.90	19.20	9.34	4.17	93.46
137	U	278.16	149.75	7.40	3.27	.52	94.10
138	U	287.79	164.28	3.84	1.70	.18	94.75
139	U	.00	174.61	2.33	1.10	.11	95.39
140	U	67.78	163.86	1.64	.80	.08	96.04
141	U	76.82	149.33	1.36	.63	.05	96.68
142	U	79.70	134.53	1.50	.70	.04	97.32
143	U	80.82	119.68	2.12	1.00	.05	97.97
144	U	80.42	104.80	3.77	2.13	.13	99.26
145	L	80.10	90.00	1.68	7.19	.91	99.90
146	L	79.09	75.26	2.44	8.62	1.53	100.55
147	L	77.13	60.63	2.78	6.95	1.59	101.19
148	L	73.49	46.21	2.75	5.88	1.52	101.84
149	L	66.12	32.27	2.30	4.81	1.29	[illegible]
150	L	47.98	19.83	1.55	[illegible]		
151	L	[illegible]			[illegible]	.19	165.00
			[illegible]	4.15	1.95	.17	165.00
[illegible]	U	3.97	104.48	3.64	1.78	.14	165.00
261	U	7.63	102.95	3.62	1.88	.13	165.00
262	U	10.73	100.55	4.15	2.29	.16	165.00
263	U	13.06	97.44	4.26	2.93	.24	165.00
264	U	14.51	93.84	3.49	4.30	.45	165.00

"nadir" ground pixel

ground

horizon pixel

sky

horizon pixel

direct beam of sun = detector saturation w/o N.D. filter

********** TAPE ID = 83-0

ID # : 13 DAY : 225 TIME 9:02 DATE : 08-10-83

TEMPERATURE (DEG. CENTIGRADE)

DETECTOR 1	DETECTOR 2	DETECTOR 3	HOUSING
19.53	19.53	4.69	26.17
20.31	20.31	5.08	25.39
20.31	20.70	5.08	25.39

Figure B-4. Standard computer listing (partial) of computed radiances and viewing angles for a typical PARABOLA scan and showing header (identification) and temperature records.

SKY HEMISPHERE — "TUFTED" ORCHARDGRASS SITE

AUGUST 10, 1983 9:05 am EDST

PARABOLA CHANNEL 2 (.826 μm) RADIANCE (mW/cm²/μm/ster.)

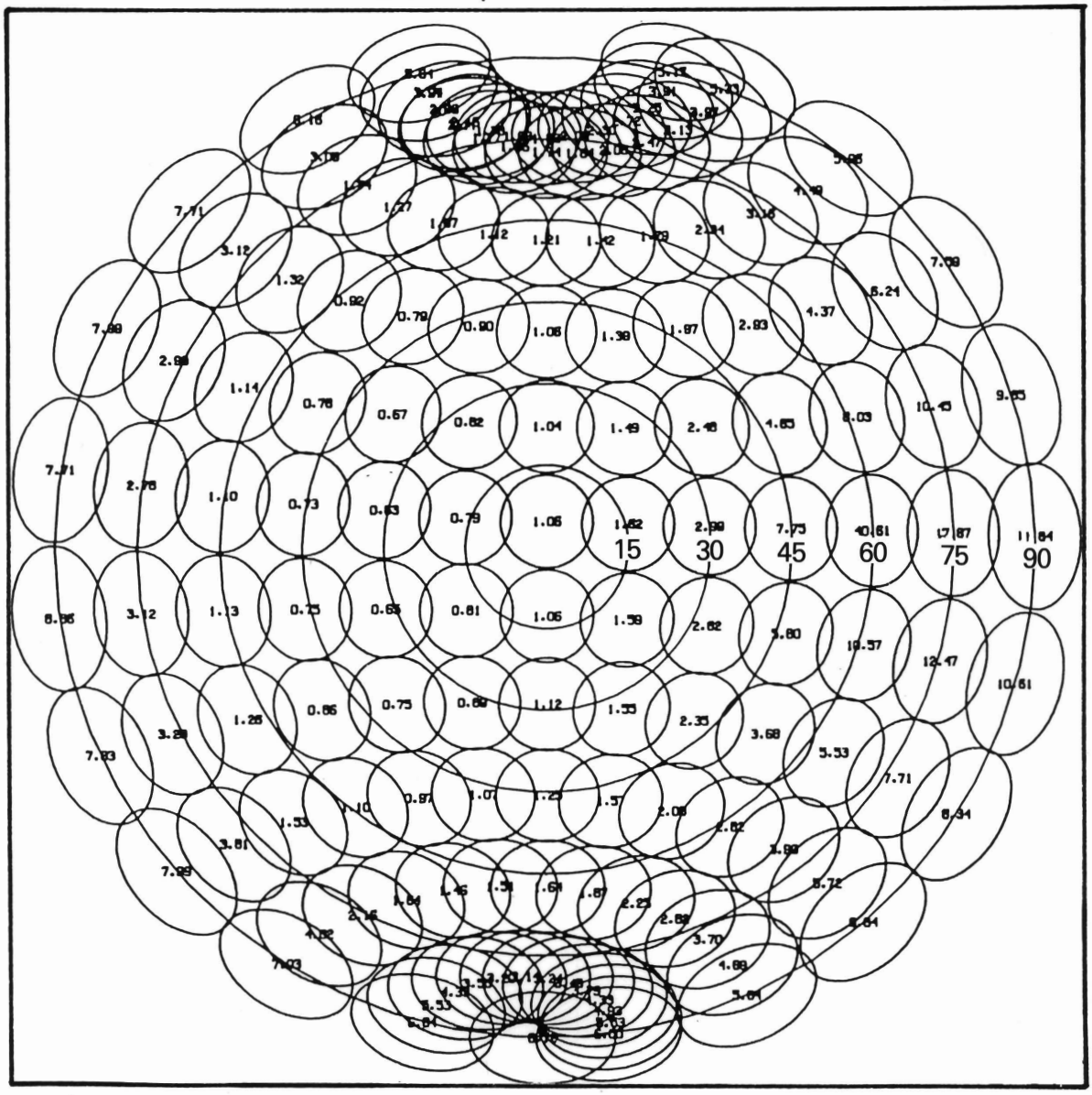

PARABOLA RUN NO. 83-015

Figure B-5a. Clear sky radiance measurements for Channel 2 over an orchardgrass field as spatially distributed on a sky hemisphere IFOV pixel print.

"TUFTED" ORCHARDGRASS CANOPY — GROUND HEMISPHERE

AUGUST 10, 1983 9:05 am EDST

PARABOLA CHANNEL 2 (.826 μm) RADIANCE

(mW/cm²/ μm/ster.)

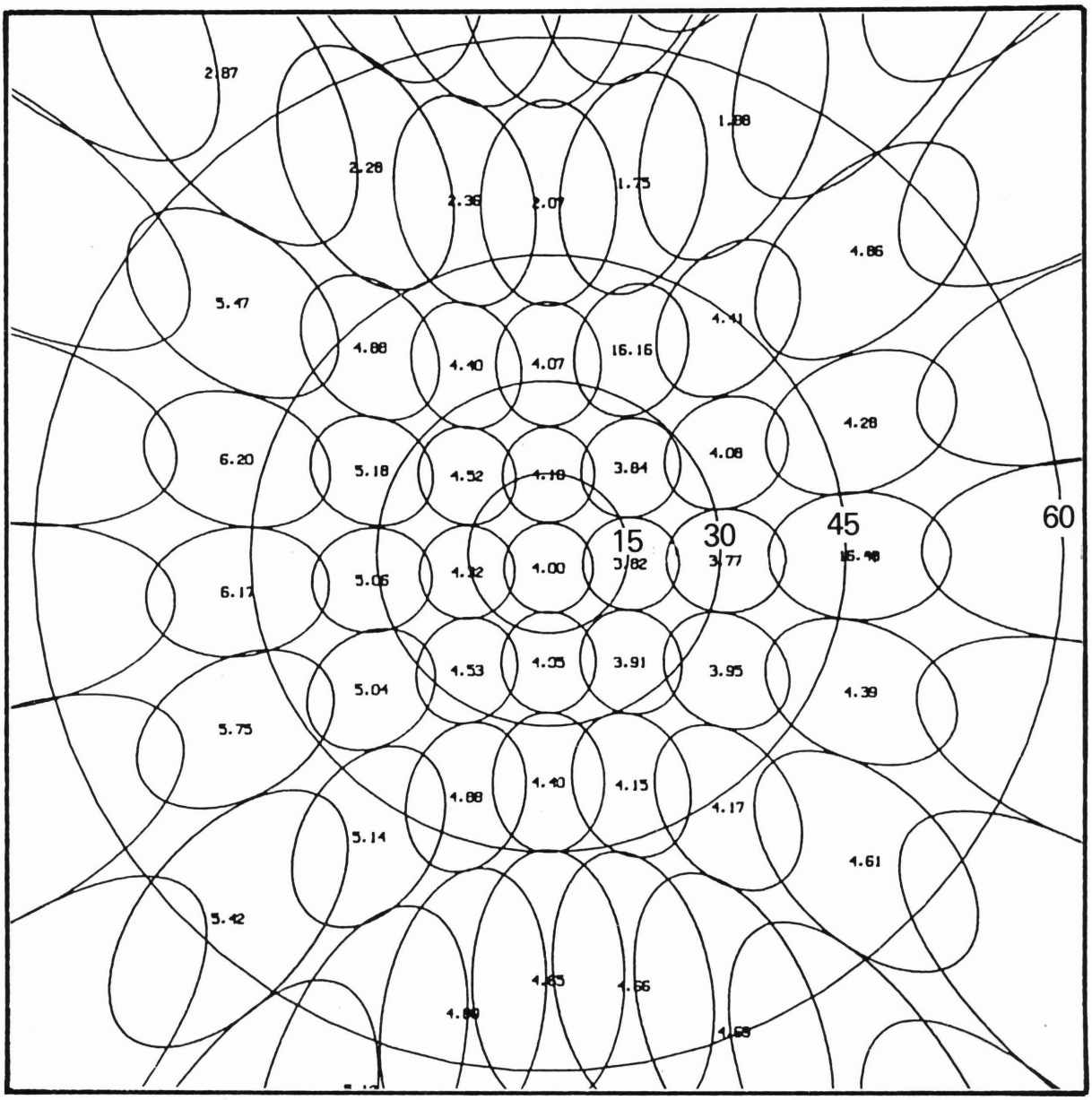

PARABOLA RUN NO. 83-014,15,16

Figure B-5b. Channel 2 ground hemisphere radiances (means from three samples) of an orchardgrass canopy as spatially distributed on a ground hemisphere IFOV pixel print.

"TUFTED" ORCHARDGRASS CANOPY — GROUND HEMISPHERE

AUGUST 10, 1983 9:05 am EDST

PARABOLA CHANNEL 1 (.662μm) REFLECTANCE FACTORS

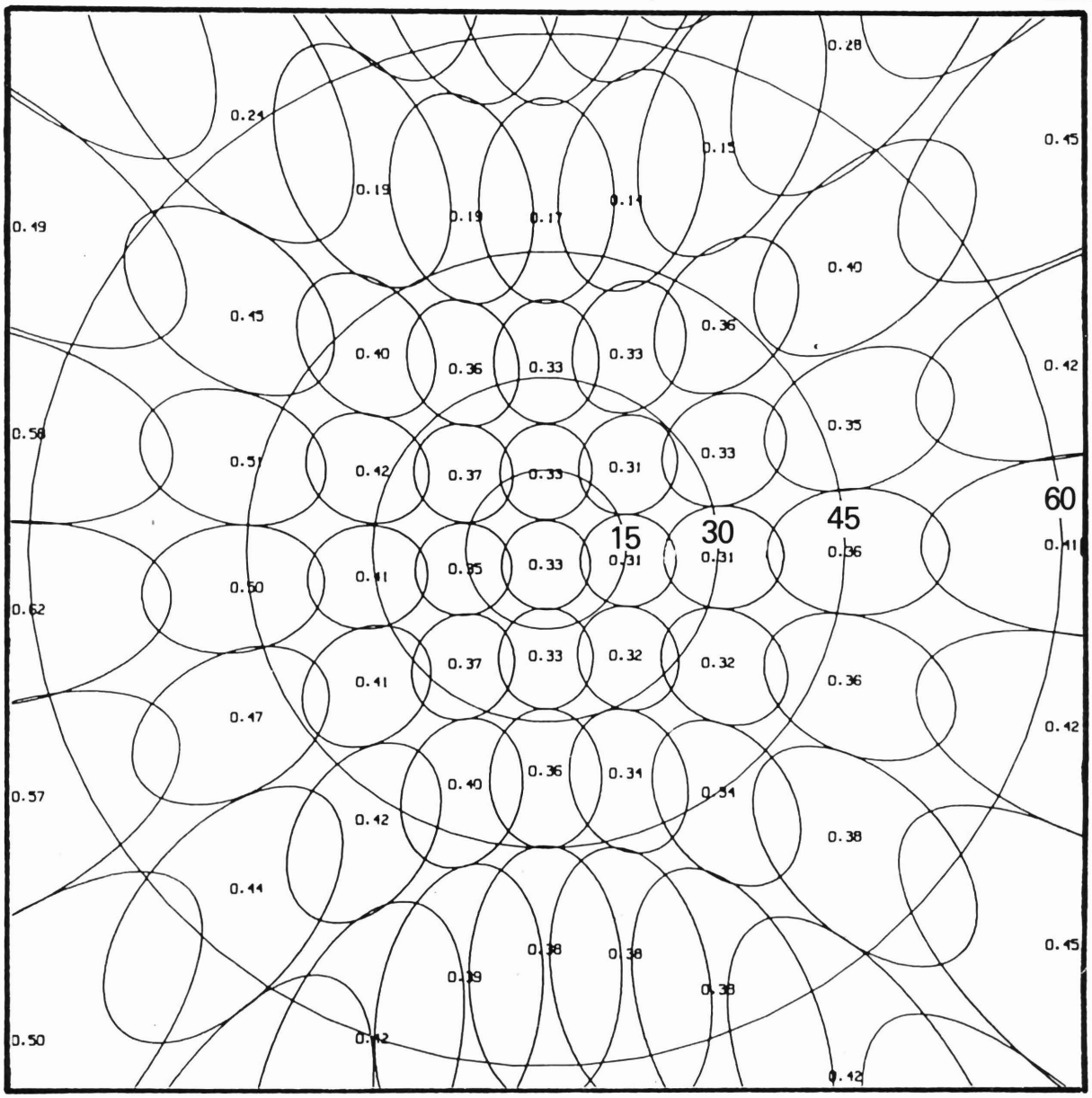

PARABOLA RUN NO. 83-014,15,16

Figure B-5c. Channel 1 ground hemisphere radiances (means from three samples) of an orchardgrass canopy as spatially distributed on a ground hemisphere IFOV pixel print.

INTERPOLATION PROCEDURE FOR PRINCIPAL PLANE VALUES*

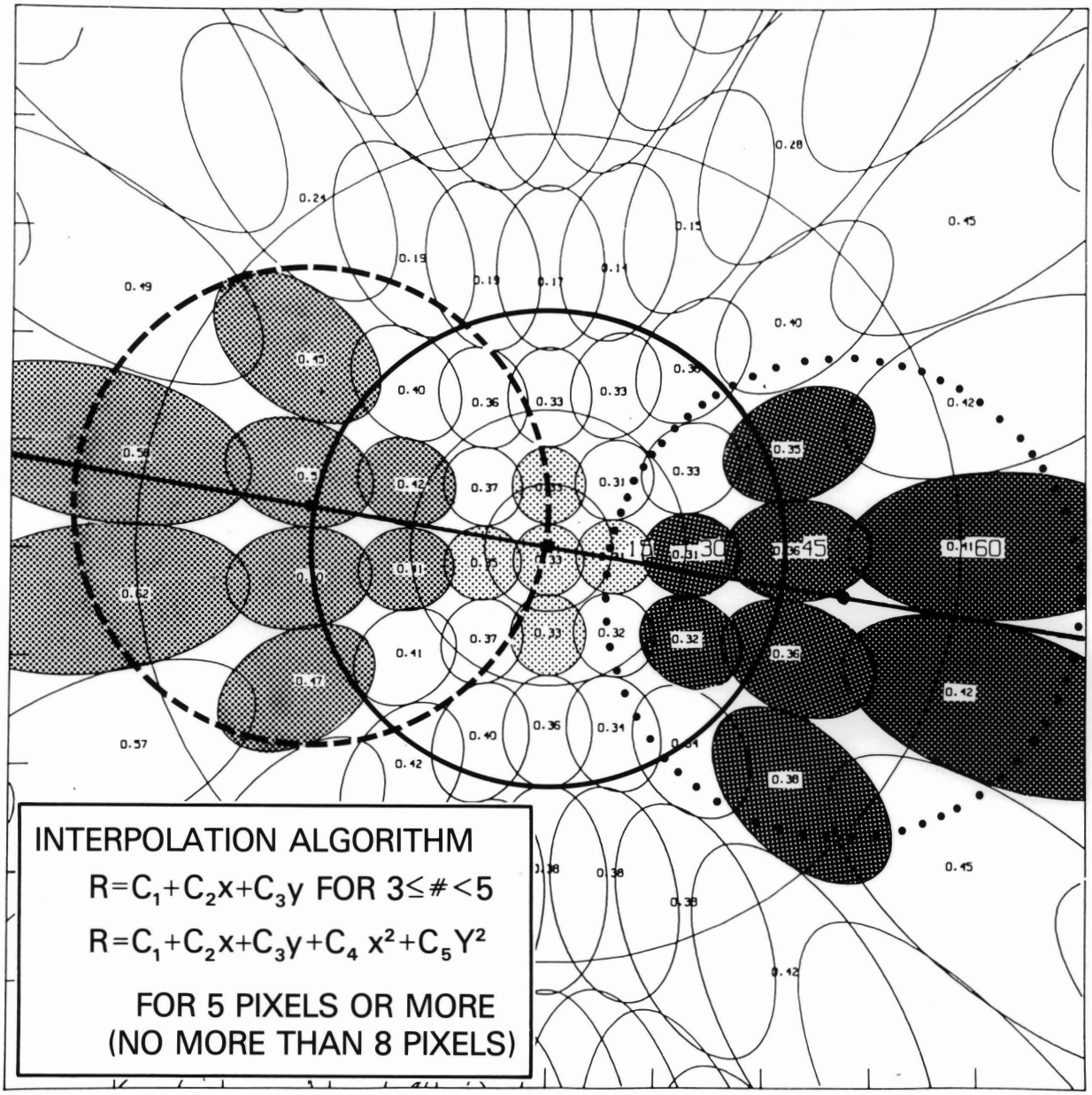

*EXAMPLE FOR THREE VIEW ANGLES

Figure B-6a. Interpolation procedure for azimuthal transects through a PARABOLA data set.

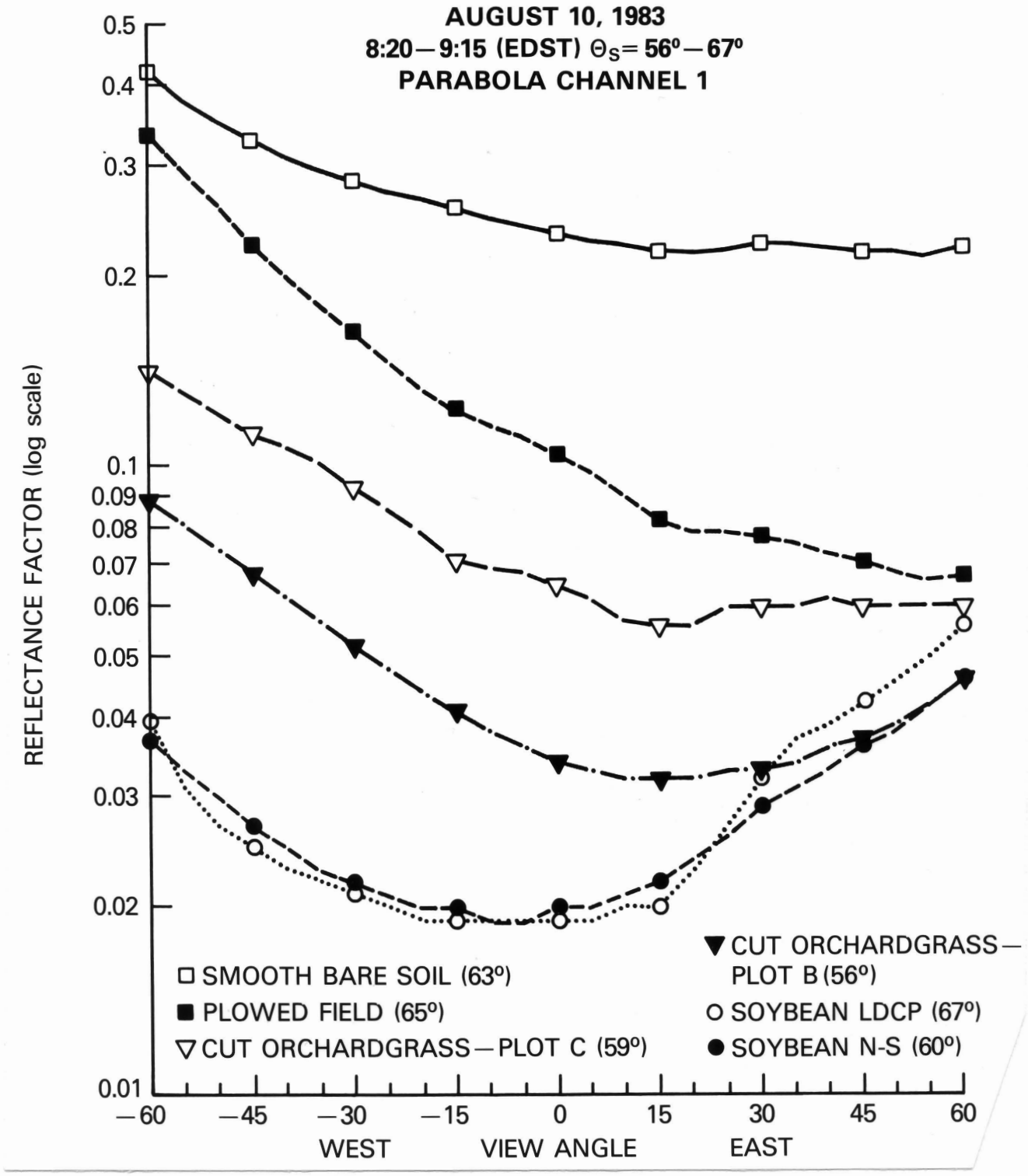

Figure B-6b. Graph of solar principal plane ground reflectances as computed for PARABOLA Channel 1 for three surface cover types (note Y-axis is log scale).

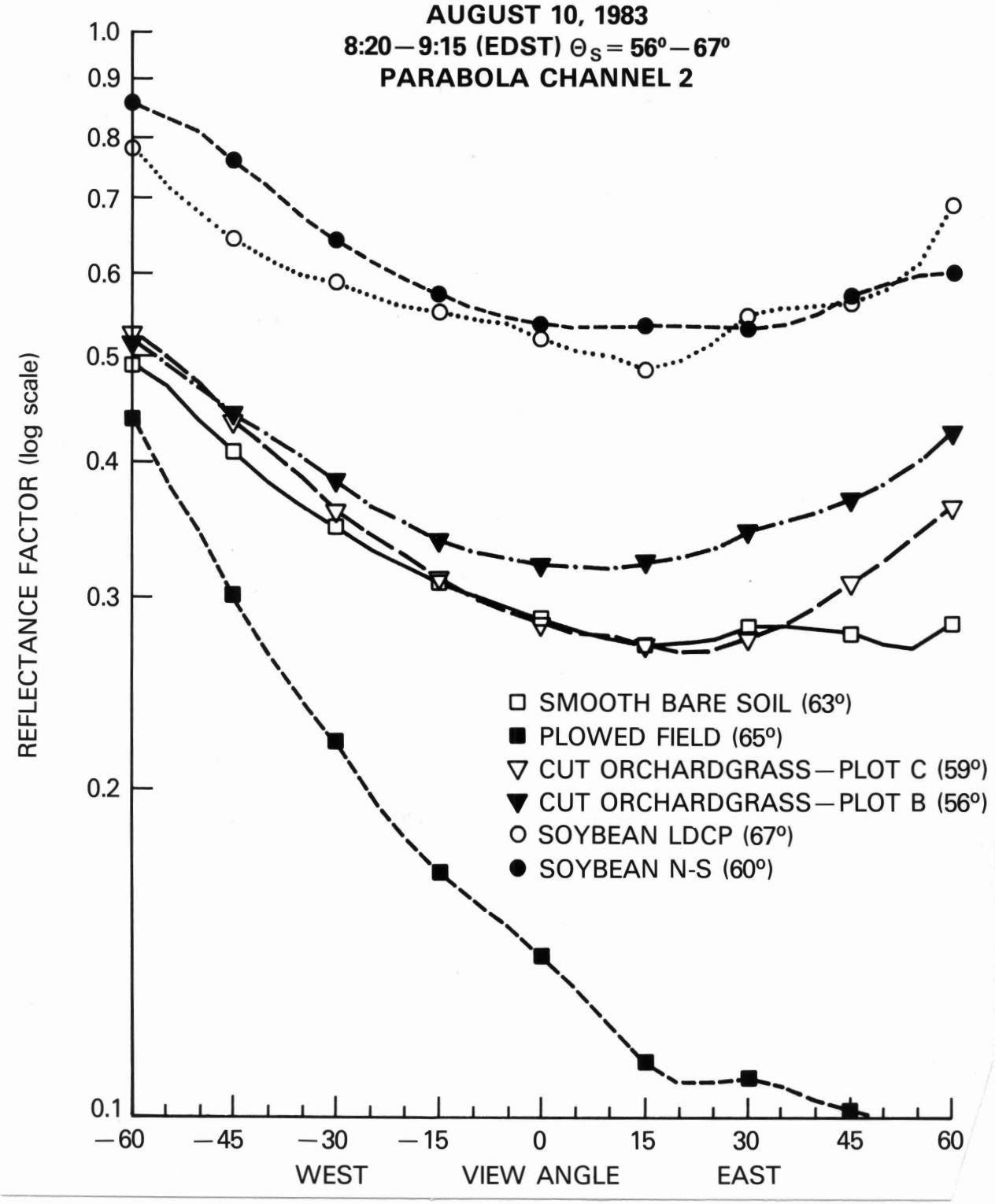

Figure B-6c. Graph of solar principal plane ground reflectances as computed for PARABOLA Channel 2 for three surface cover types (note Y-axis is log scale).

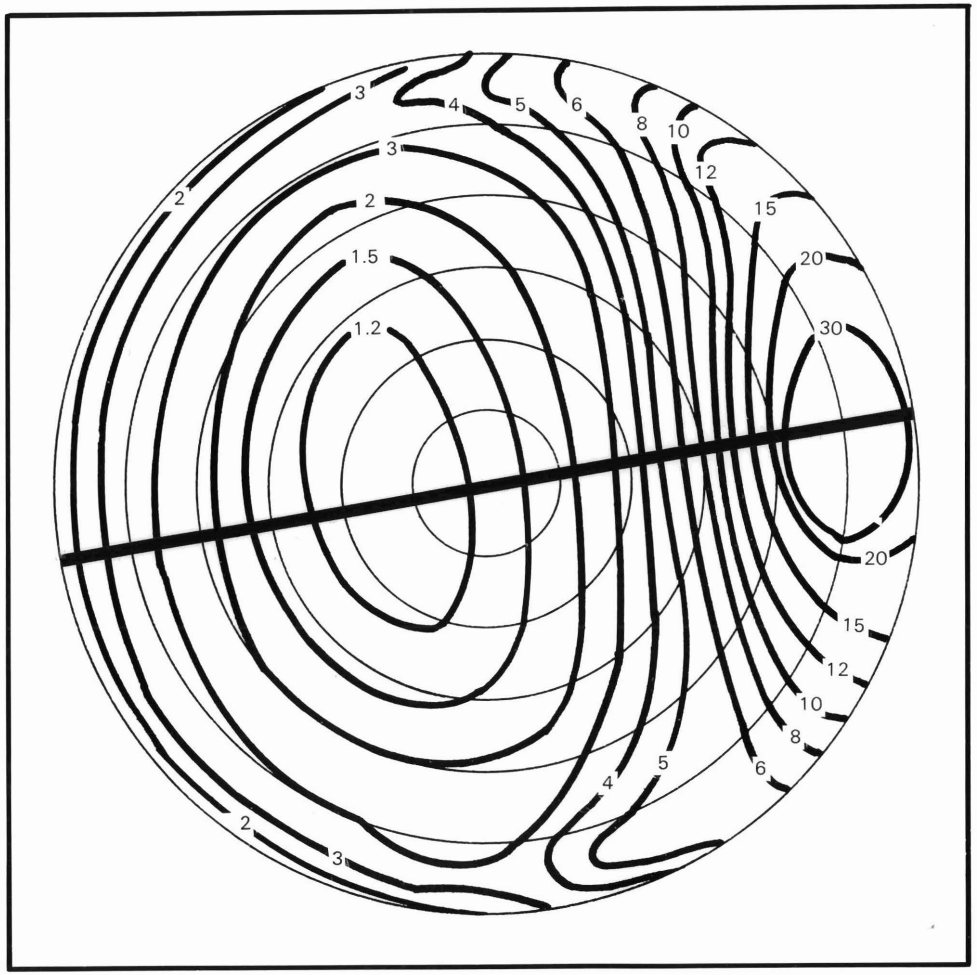

PARABOLA
CHANNEL 1 (.662μm)
RADIANCES
(mW/cm^2/μm/ster.)

AUGUST 10, 1983
(CLEAR SKY)

7:51 a.m. EDST
($\Theta_s = 73°$, $\Phi_s = 83°$)

TUFTED

ORCHARDGRASS

SITE

Figure B-7a. Isolines of sky radiance distribution from PARABOLA Channel 1 data set: early morning (low sun elevation) example (transect line is solar plane).

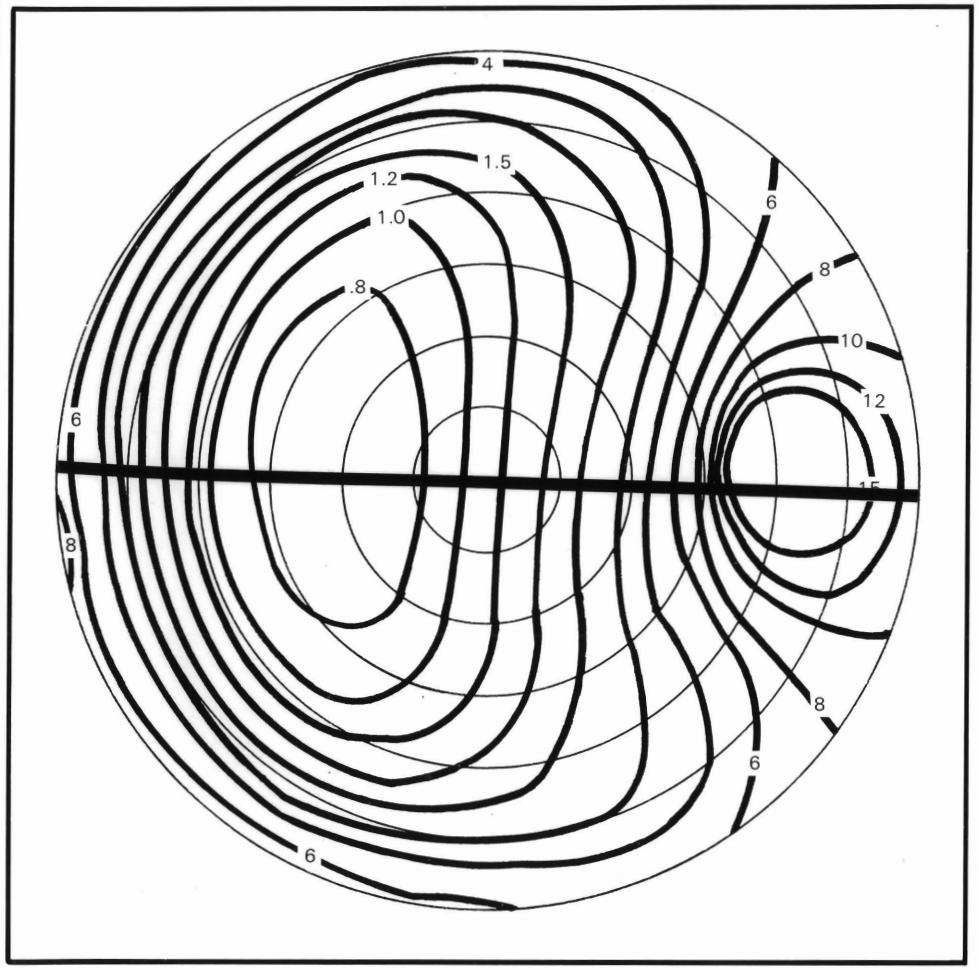

PARABOLA
CHANNEL 2 (.826μm)
RADIANCES
(mW/cm^2/μm/ster.)

AUGUST 10, 1983
(CLEAR SKY)
9:05 a.m. EDST
($\Theta_s = 59°$, $\Phi_s = 95°$)

TUFTED

ORCHARDGRASS

SITE

Figure B-7b. Isolines of sky radiance distribution from PARABOLA Channel 2 data set: early morning (low sun elevation) example (transect line solar plane).

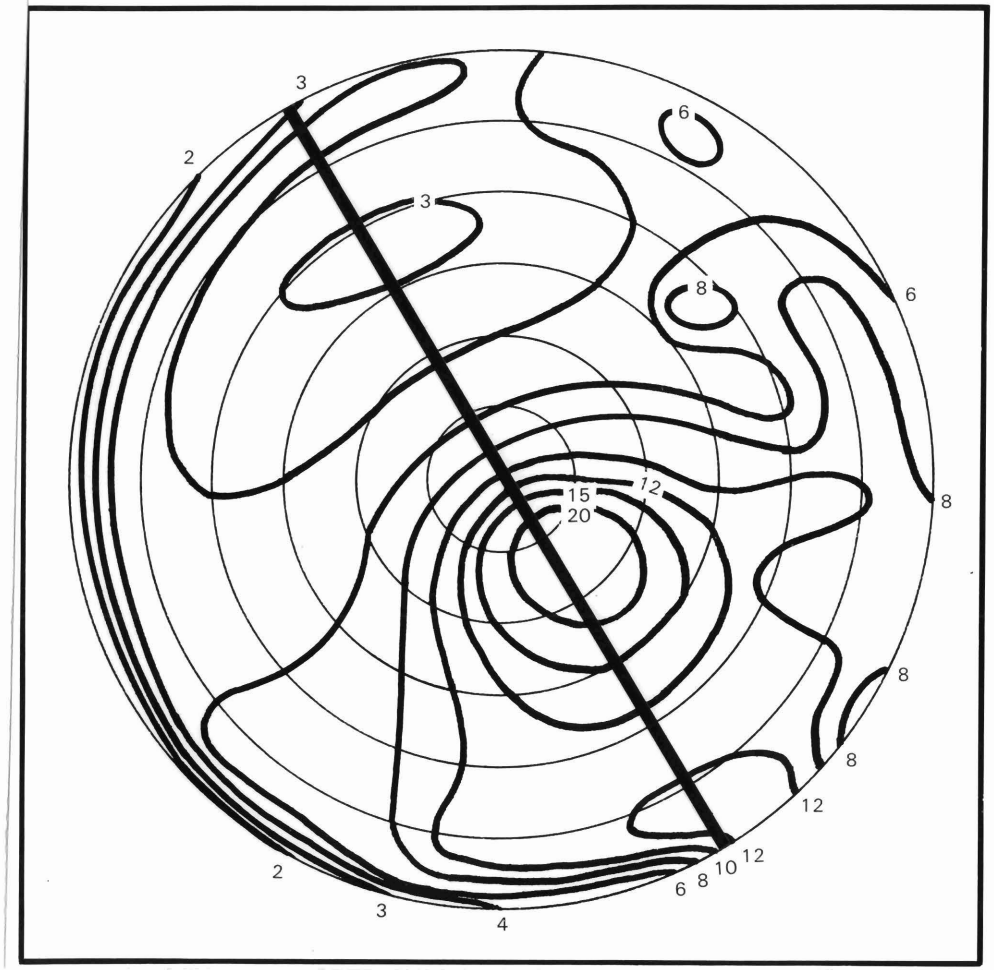

PARABOLA
CHANNEL 1 (.662 μm)
RADIANCES
(mW/cm^2/μm/ster.)

AUGUST 10, 1983
(CLEAR SKY)

12:24 p.m. EDST
($\Theta_s = 25°$, $\Phi_s = 152°$)

PLOWED FIELD SITE

Figure B-7c. Isolines of sky radiance distribution from PARABOLA Channel 1 data set: near noon (high sun elevation) example (transect line is solar plane).

SKY HEMISPHERE RADIANCES — TUFTED ORCHARDGRASS SITE

9:05 a.m. EDST ($\Theta_s = 59°$, $\Phi_s = 95°$)

AUGUST 10, 1983 (CLEAR SKY)

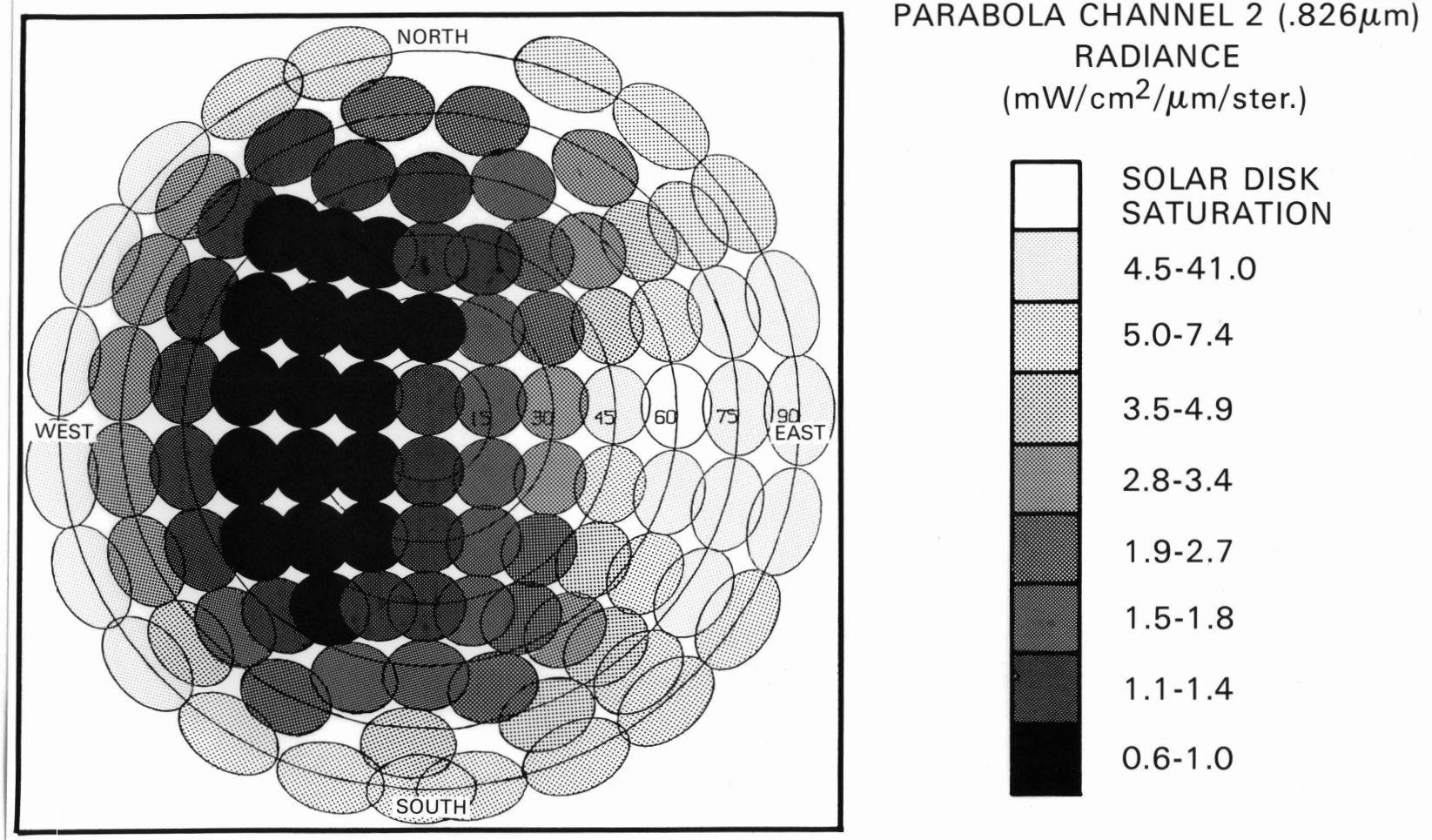

Figure B-8. Grey-tone representation of a sky radiance distribution for PARABOLA Channel 2 (see also Figure A-7b).

BARE SOIL SURFACE AND WEST-EAST CROSS SECTION RADIANCES

10:03 a.m. EDST ($\Theta_s = 40°$, $\Phi_s = 109°$) — FRESHLY PLOWED FIELD

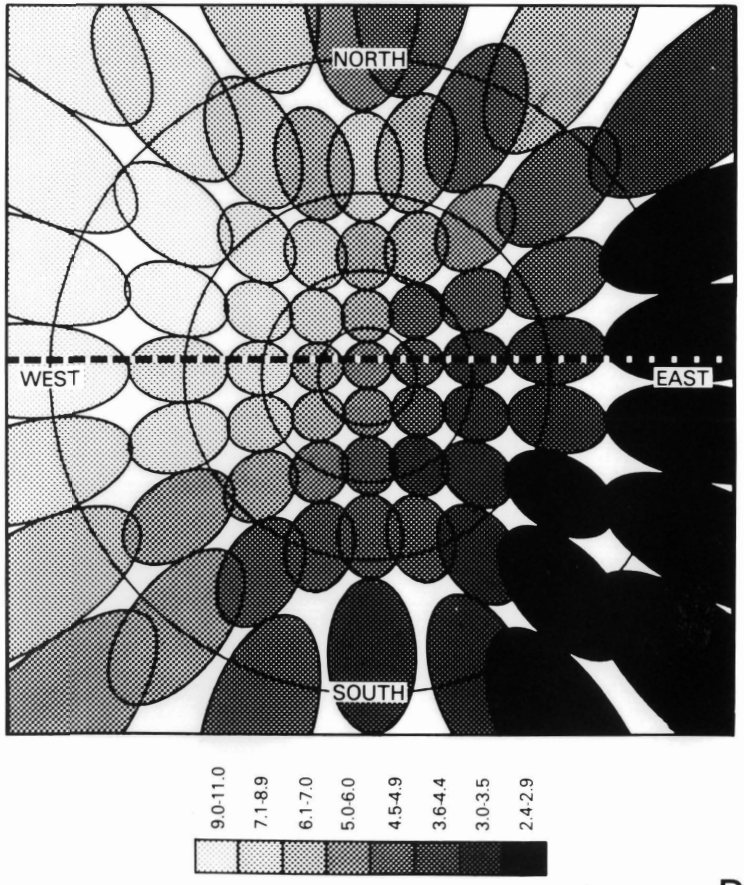

AUGUST 19, 1982 (CLEAR SKY)

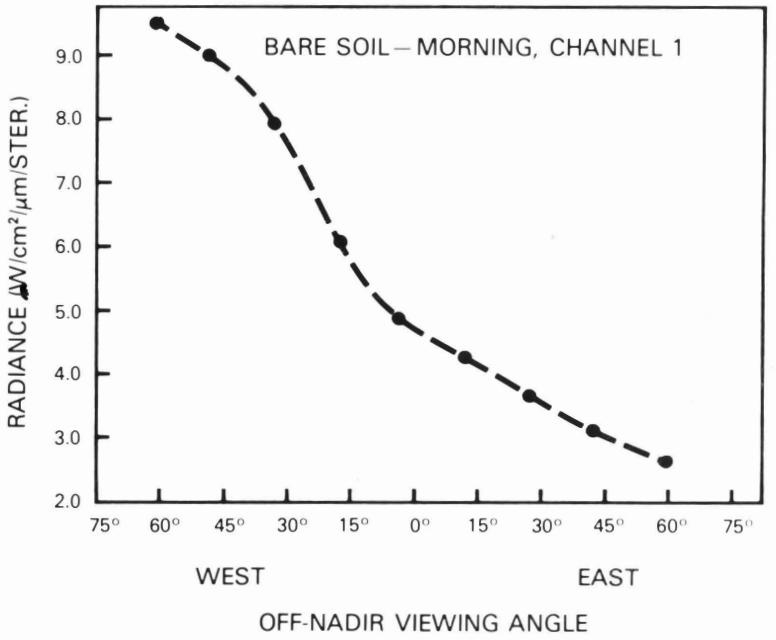

PARABOLA CHANNEL (.65-.67μm) RADIANCE IN mW/cm²/μm/STER.

Figure B-9a. Grey-tone ground footprint representation of PARABOLA Channel 1 radiance for a plowed field.

SOYBEAN FIELD AND PRINCIPAL PLANE CROSS SECTION MEAN RADIANCES

10:16 ~ 10:32 a.m. EDST ($\Theta s = 45°$, $\Phi s = 113°$)

AUGUST 16, 1982 (CLEAR SKY)

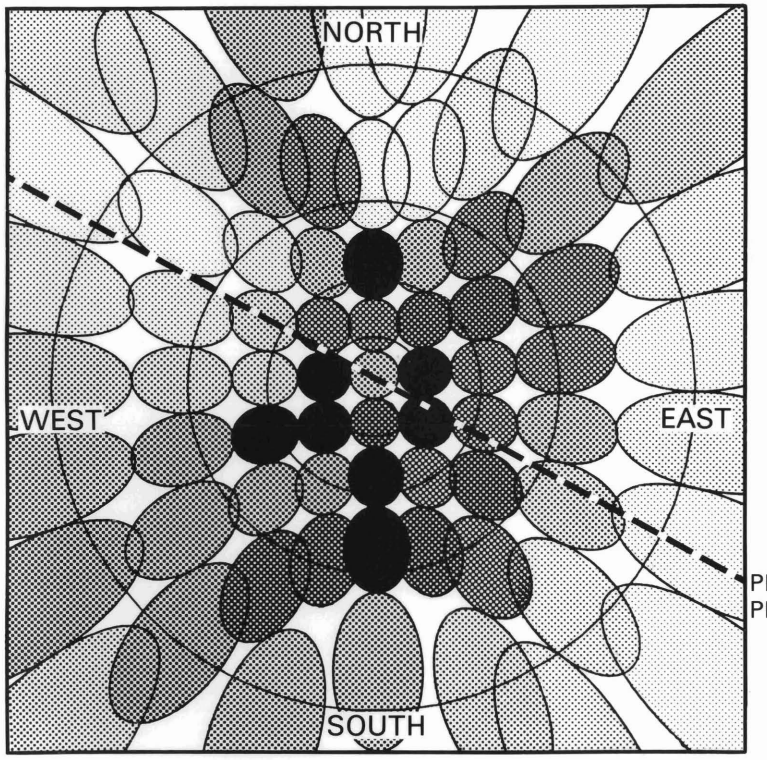

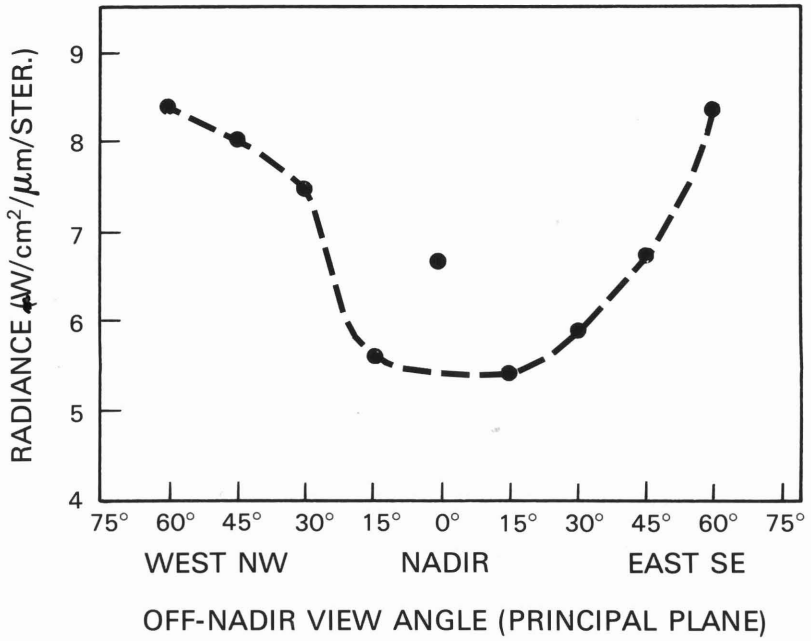

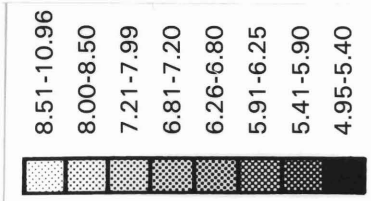

PARABOLA CHANNEL 1 (.65-.67μm)
RADIANCE IN mW/cm²/μm/STER.

Figure B-9b. Grey-tone ground footprint representation of PARABOLA Channel 1 radiance for a soybean field.

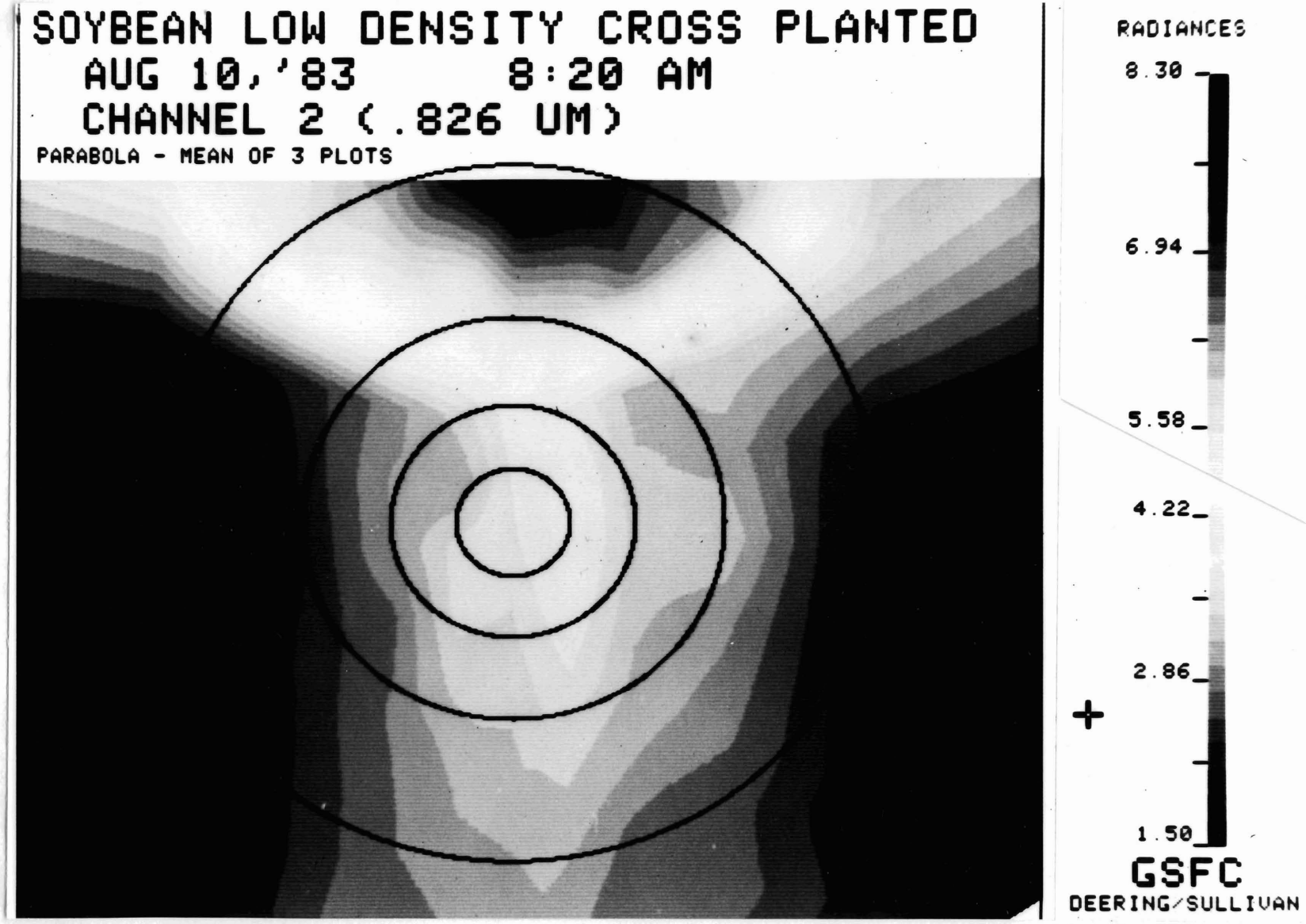

Figure B-10. Color computer monitor display of a soybean canopy directional radiance distribution computed from PARABOLA Channel 2 data (note 15° increment off-nadir viewing "bullsize" superimposed for reference, also note influence of instrument support van on the top (north) side at >45° viewing angle.

APPENDIX C

PARABOLA INSTRUMENT GEOMETRIC CHARACTERISTICS SOFTWARE USER'S GUIDE

April 1983

Prepared for:

National Aeronautics and Space Administration
Goddard Space Flight Center
Greenbelt, Maryland 20771

Prepared by:

J. Park
T. Ostroff

Systems and Applied Sciences Corporation
6811 Kenilworth Avenue
Riverdale, Maryland 20737

PARABOLA INSTRUMENT GEOMETRIC CHARACTERISTICS
SOFTWARE USER'S GUIDE

TABLE OF CONTENTS

Appendices
--------- (NOT INCLUDED IN THIS NASA TM) ---------

Figures

Tables

1 - GENERAL INFORMATION

1.1 Instrument Overview

The PARABOLA (Portable Apparatus for Rapid Acquisition of Bidirectional Observations of Land and Atmosphere or Bidirectional Reflectance Field Instrument) is a portable instrument designed by GSFC scientists and engineers. It can spatially scan nearly a full sphere, measuring incident (sun and sky) and reflected (ground) radiation in three spectral bands (.65-.67μm, .81-.84μm, and 1.62-1.69μm). In use, the scan head is positioned on a horizontal boom over the ground to be scanned. Normal IFOV of the sensor is 15^{o} and scan cycle time is 11 sec. During the data acquisition cycle the scan head rotates at 360 deg/sec about an axis parallel to the support pipe, while at the same time tilting at a rate of 15 deg/sec about the orthogonal horizontal axis. Sampling is done in a continuous helical pattern at every 15 degree increment of the roll angle (Figure 1.1).

1.2 Software Overview

A series of computer programs were written to support the operation of the PARABOLA instrument. These programs were needed to examine the geometric characteristics of the sensors footprints on the ground sufrace and the sky when the instrument sensors scanned the ground surface and the sky. In the analysis of the data measured by the instrument which and how large areas the sensor really looked at, it is desired to know where the overlapped portions of the footprints were located in the string of the data and which portions of the sphere were not covered by the sensors. Individuals programs were designed to:

- Compute view angle differences between any two samples pixels* (see Section 2.2). The program calculates the arc distance between any two pixels.

- Compute fractional overlap areas between sensor fields of view (2.3). The program calculates the area percentage overlap between any two pixels.

Note*: Pixel stands for picture element. Following the recent remote sensing terminology a "pixel" used here is a sample scanned for one spot by the instrument.

- Select optimum samples in order to reduce overlapped areas between IFOV's of the Samples (2.9). The program has the option of selecting maximum overlap percentage and listing all pixel pairs falling in each percentage category.

- Compute off-nadir angle and azimuth of the sensor for each sample data (2.4). The program calculates the off-nadir angle and azimuth angle for each sample data.

- Compute major and minor axes, and center location of the off-nadir view footprint ellipse (2.5). The program calculates the half major and half minor axes and the center locations of the ellipses.

- Draw footprint ellipses on the ground surface (2.6)

- Draw unit circles representing 15^{o} IFOV appropriately located in the upper hemisphere (2.7).

- Draw sensor patterns in the azimuthal equidistant projection (2.8)

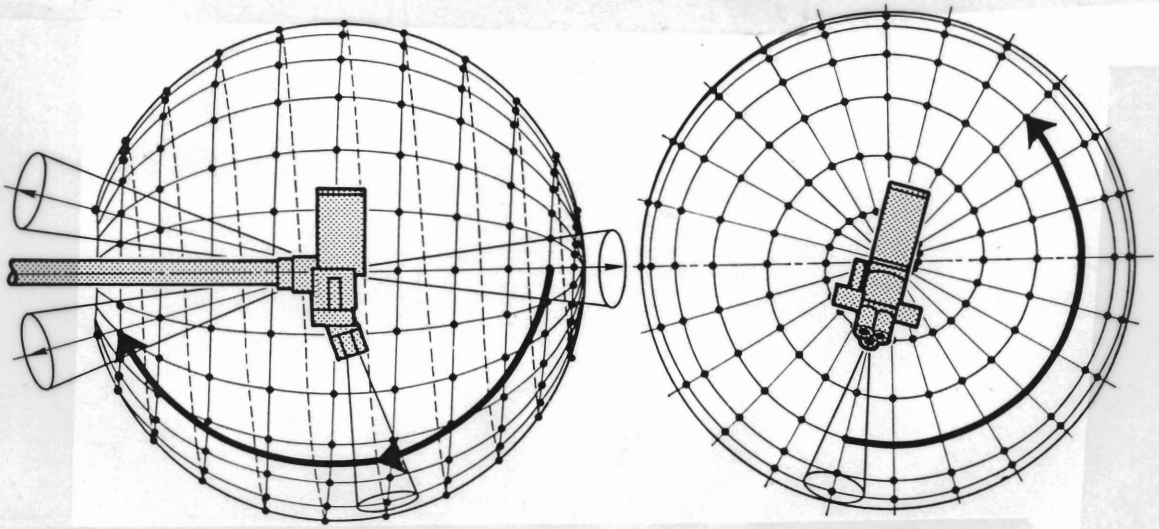

Figure 1.1

2. MATHEMATICAL EXPRESSIONS OF VARIABLES/PARAMETERS

2.1 Sensor Locations

The first step for the tasks stated in the previous section is to properly define the sensor motion in terms of mathematical functions and to locate the center of the sensors IFOV in the appropriate coordinate system. The spherical coordinate is the most appropriate one for this purpose, since the sensor head continuously rotates showing a helical pattern. It is defined that the sensor initially directs toward the positive Z-axis and starts moving from the X-Z plane. And the two angles of the coordinate system are measured as shown in Figure 2.1. Then, the sensor motion can be described in accordance with the instrument specifications as follows:

Scan Rate

$\dot{\theta}$ = 15 degree/sec (elevation angular speed)
$\dot{\phi}$ = 360 degree/sec (rolling angular speed)
Δt = 1/24 sec (sampling interval)

IFOV

α = 7.5 deg (half of IFOV)

Therefore sensor elevation and rolled angles, respectively, for the ith sample are given by

$$\theta_i = \dot{\theta} t_i$$
$$\phi_i = \dot{\phi} t_i$$

where

$$t_i = \Delta t\ (i-1)$$
$$i = 1,2,3,\ldots,264 \quad \text{(sample number)}$$

2.2 Angular Distance Between Two Samples

The angular distance between two samples is an important parameter as a measure of their separation and in the calculation of the overlap by the two IFOVS. In the

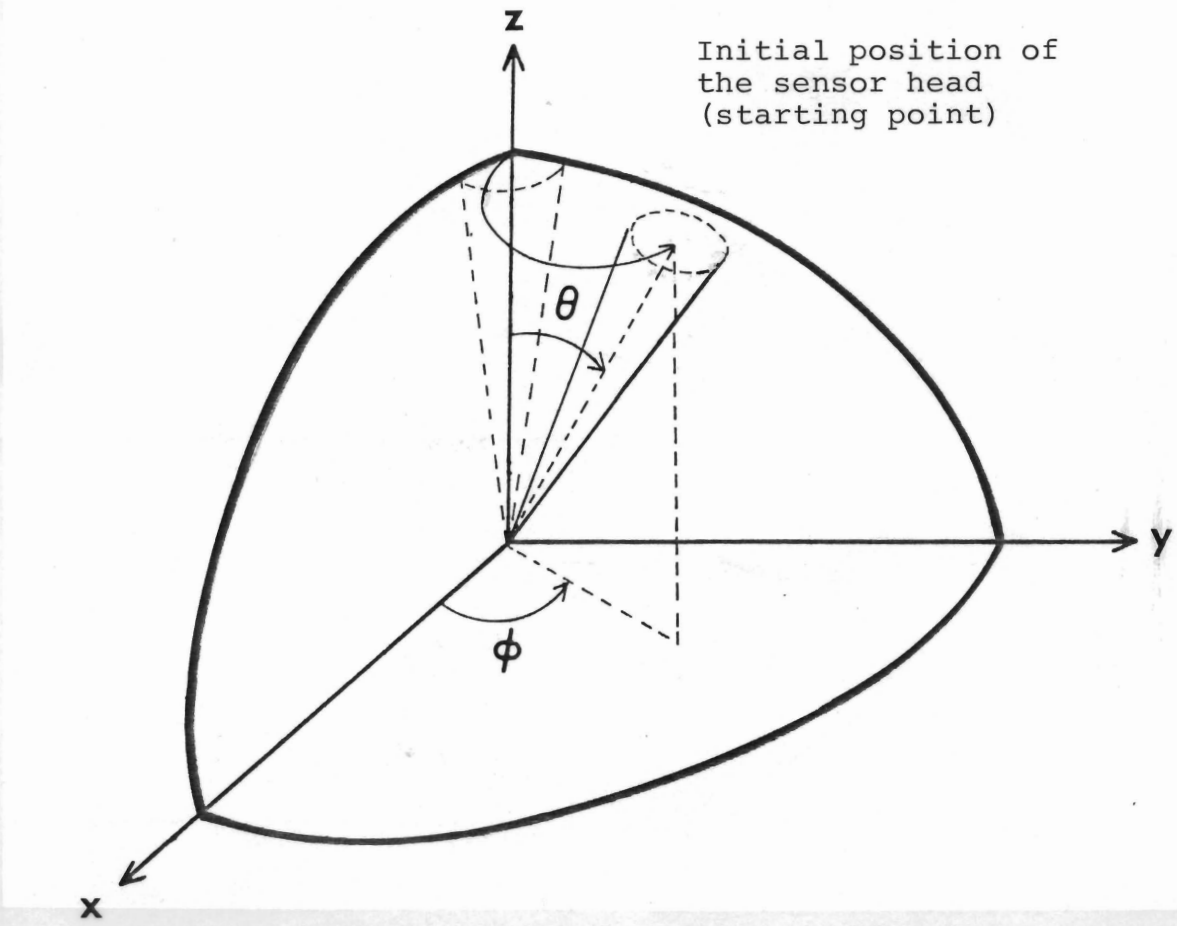

Figure 2.1 Spherical Coordinate System Defining the Location of the PARABOLA Sensor Center Point (here showing a 1/8 unit sphere).

spherical coordinate system the difference between the i-th and j-th samples is computed by

$$\delta_{ij} = \cos^{-1}(\sin\theta_i \cos\phi_i \sin\theta_j \cos\phi_j + \sin\theta_i \sin\phi_i \sin\theta_j \sin\phi_j + \cos\theta_i \cos\theta_j)$$

2.3 Overlapped Areas and Optimum Sample Selection

Overlaps among field-of-views of any samples occur if their separation (δ_{ij}) is smaller than the angle of the sensor IFOV. The fractional overlap area between two samples i and j can be approximated by

$$O_{ij} \approx \frac{2}{\pi} \cos^{-1} X_{ij} - X_{ij} \left(1 - X^2_{ij}\right)^{1/2}$$

where

$$X_{ij} = \begin{cases} 0 & \text{if } \delta_{ij} > 2\alpha \\ \dfrac{\delta_{ij}}{2 \sin \alpha} & \text{if } \delta_{ij} << 2\alpha \\ \dfrac{\delta_{ij}}{2\alpha} & \text{if } \delta_{ij} \leq 2\alpha \end{cases}$$

This approximation is good only for small α (far less than $\pi/2$).

In the PARABOLA scanning pattern there are multiple overlaps of individual IFOV's at the beginning and the end sequence of a sampling run. It is desirable to minimize mixed and/or overlapped areas of the samples to be analyzed because:

- o mixed views of sky and ground portions might lead to wrong interpretations of the radiation distribution.

- o only one representative sample might be enough in the overlapped portions for analysis.

Hence, optimum samples might be selected by eliminating redundant coverages over the same area and by taking out any suspicious samples such as first several ones. In the optimum selection program, selection criteria are defined by

$$i \geq i_c$$
$$O_{ij} < O_c$$
$$i \neq (i_1, i_2, \ldots, i_k)$$

where i and j are subscripts indicating selected samples, the first sample to be selected, O_c, the minimum overlap fraction between two samples, and $(i_1, i_2, \ldots, i_k)$ samples are to be excluded.

2.4 Sensor Off-Nadir Angle and Azimuth

The relative position of the PARABOLA sensor in motion is given by the equation of motion described in Section 2.1. But the sensor position defined in terms of elevation and roll angles has to be converted into off-nadir angle and azimuth in order to examine which parts of the ground surface or the sky are being scanned at each time. It is also desirable to know the off-nadir angle and azimuth of the sensor for proper interpretation of radiance measurements, since the angles are commonly used in remote sensing communities. When the PARABOLA sensor is set up facing the south horizon before the scanning, off-nadir view angle and azimuth are given by (Figures 2.2 and 2.3)

$$\eta_i = \cos^{-1}(\sin\theta_i \sin\phi_i)$$

$$\xi_i = \pi - \tan^{-1}\left(\frac{1}{\tan\theta_i \cos\phi_i}\right)$$

In this equation the sensor azimuth is measured counterclockwise* from the north horizon. To get correct quadrangles in the azimuth computation, it is computed by

$$\xi_i = -\text{ATAN2}(\sin\theta_i \cos\theta_i, \cos\theta_i)$$

on the IBM computer. Note(*) that the sensor azimuth is often measured clockwise from the north horizon, which causes additional computations in applying to conventional mathematical formulae and hence is not adopted in this guide.

2.5 Footprint Ellipses

The footprint viewed by an off-nadir sensor is an ellipse, parabola or hyperbola depending on its view angle. If the off-nadir view angle η is less than $\pi/2-\alpha$, it will be an ellipse (Figure 2.4), whose major and minor axes are given by

Figure 2.2

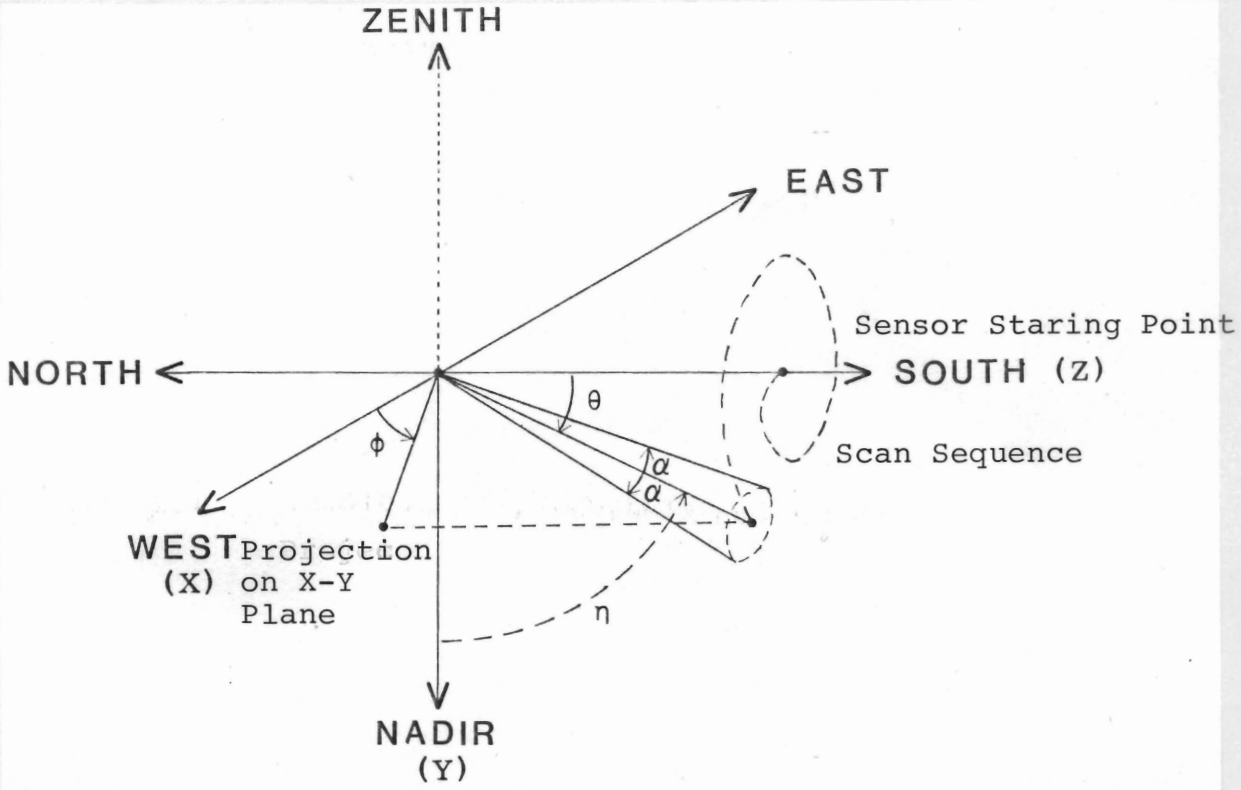

Figure 2.2 Illustration of Sensor Off-Nadir Angle (η_i) when the Sensor Starting Point is Facing Toward the South Horizon

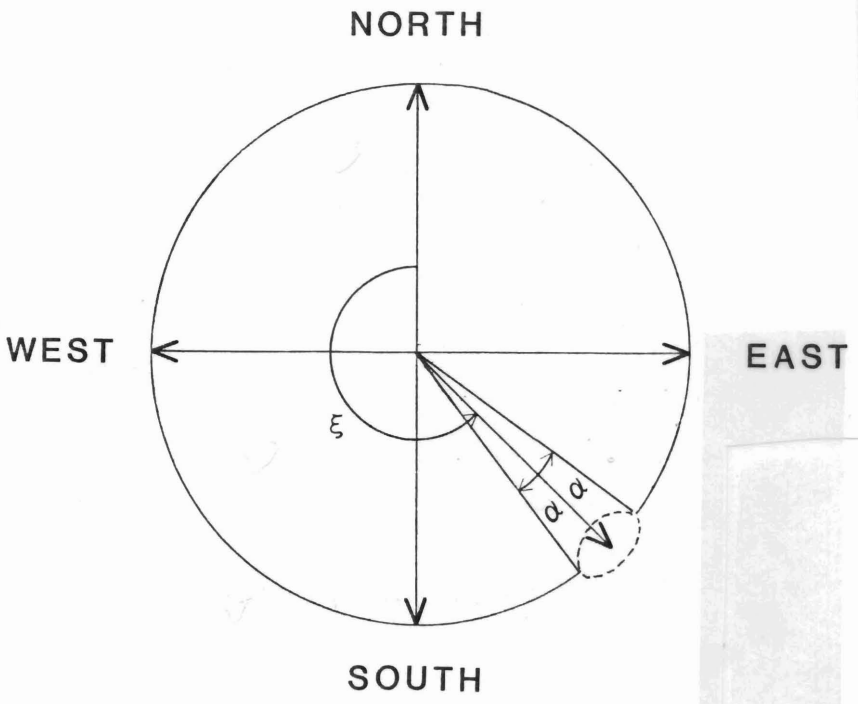

Figure 2.3 Sensor Azimuth (shown in the horizontal plane) Measured Counterclockwise from the North Horizon.

$$a_i = \frac{H \tan\alpha(1 + \tan^2\eta_i)}{1 - (\tan\alpha \tan\eta_i)^2}$$

$$b_i = \frac{H \tan\alpha}{\cos\eta_i \left[1 - (\tan\alpha \tan\eta_i)^2\right]^{1/2}}$$

where

H = sensor height

$$\eta_i < \frac{\pi}{2} - \alpha$$

Then, the area of the elliptic footprint can be computed by

$$A_i = \pi a_i b_i$$

The ratio area of the ellipse to nadir-viewed circular footprint is given by

$$R_i = \frac{1 + (\tan\eta_i)^2}{\cos\eta_i \left[1 - (\tan\alpha \tan\eta_i)^2\right]^{3/2}}$$

When the X-Y coordinate is defined at the center of the nadir-viewed circle, the center of the footprint ellipse is located at

$$X_c = \left[H\tan(\eta_i - \alpha) + a_i\right] \cos(\xi_i - 3\pi/2)$$

$$Y_c = \left[H\tan(\eta_i - \alpha) + a_i\right] \sin(\xi_i - 3\pi/2)$$

2.6 Drawing Parameters of Footprint Ellipses

The X and Y coordinates of the footprint ellipse are given by

$$X = X_C + r_i \cos(\xi_i - 3\pi/2) \cos\gamma - \sin(\xi_i - 3\pi/2) \sin\gamma$$
$$Y = Y_C + r_i \sin(\xi_i - 3\pi/2) \cos\gamma + \cos(\xi_i - 3\pi/2) \sin\gamma$$

respectively, where

$$r_i = a_i b_i \quad (a_i^2 \sin^2\gamma + b_i^2 \cos^2\gamma)$$

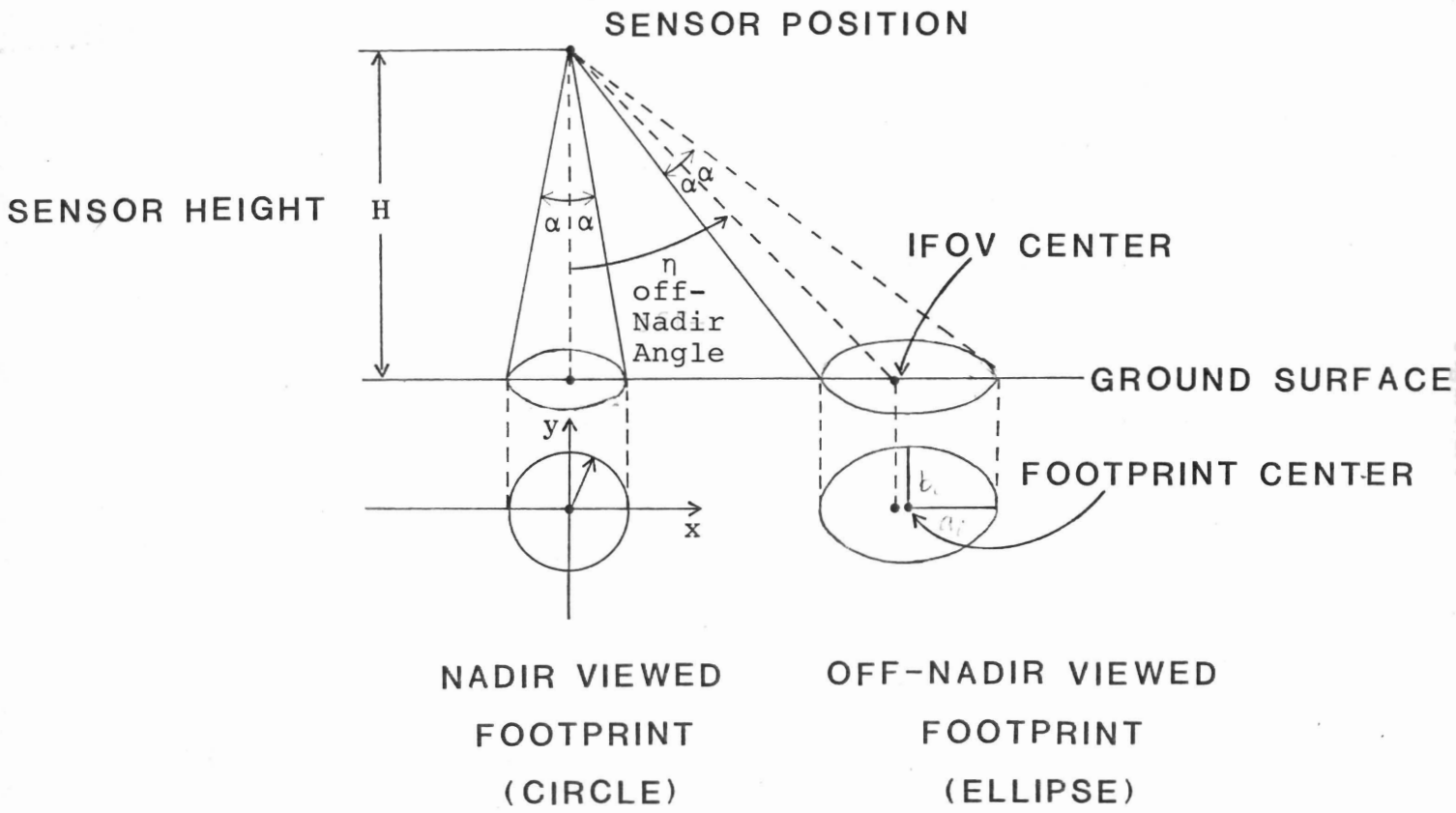

Figure 2.4 Footprints of a Sensor IFOV on the Ground

γ = angle at the ellipse center from the x- axis,

a_i and b_i as defined in Section 2.5

2.7 Drawing Parameters of Sky Scanning Patterns Using Unit Circles

Each instantaneous field-of-view of the PARABOLA sensor is a circle on the sky. All the IFOV circles in the upper hemisphere cannot be drawn on a flat paper without scale distortions. However, it might be helpful in analyzing the sensor's scanning patterns to locate each IFOV circle in a polar coordinate plot using some unit circles. For given azimuth and off-nadir angle of the sensor, the center of the IFOV circle is located at

$$X_c = f(\pi - \eta_i) \cos(\xi_i - 3\pi/2)$$

$$Y_c = f(\pi - \eta_i) \sin(\xi_i - 3\pi/2)$$

where f is a plot size parameter. A unit circle with the radius R = fα can be drawn to visualized its relative coverage in the hemisphere.

2.8 Drawing Parameters of Sky Scanning Patterns in the Azimuth Equidistant Projection

The series of all the sensor IFOV's in the upper hemisphere can be plotted in the azimuth equidistant projection, so that relative portions of sensor coverages can be easily compared with not-covered areas as well as overlapped portions. The edge of each IFOV might be described approximately by an ellipse with the half major axis and the half minor axis given by

$$a_i = R \frac{\pi - \eta_i}{\sin \eta_i}$$

$$b_i = R$$

X and Y coordinates of the ellipse can be given by the equations in Section 2.6 with the above major and minor axes.

3. PROGRAM DESCRIPTIONS

This section describes briefly each of the programs developed to fulfill the requirements specified in Section 2. Table 3.1 shows the relationship between the software developed and the algorithms defined in Section 2. For each program, the following items are described, as appropriate:

Program Overview:	Brief statement of purpose and functioning of program
Program Requirements:	Detailed requirements that the program must fulfill, including algorithms needed to implement the mathematical expressions defined in Section 2.
Data Files:	Descriptions of all input/output data files
Program Outputs:	Samples of all program outputs
Individual Routine Descriptions:	For each main program and subroutine; includes, individual variables and subroutine calling sequences

Table 3.1

Software Design to Implement Algorithm Requirements

Software	Algorithms Implemented
Angular Distances and Overlapped Areas	Sensor locations Angular distance between two samples Overlapped areas
Optimum Samples	Sensor locations Angular distances Overlapped areas Optimum sample selection
Footprint Ground Patterns	Sensor locations Sensor off-nadir angle and azimuth Parameters of footprint ellipses Plot of footprint ellipses
Sky Scanning Patterns	Sensor locations Sensor off-nadir angle & azimuth Plot of sky scanning patterns using unit circles Plot of sky scanning patterns in the azimuth equidistant projection

3.1 Angular Distance and Overlapped Areas Program

Program Overview

These programs (in FORTRAN) compute the arc distance and the overlap area between any two PARABOLA samples and output a distance matrix or overlap area matrix.

Program Requirements

Algorithm

Step 0 Read in input data: FOVANG (field of view angle)

Step 1 Compute sensor locations

$$\left.\begin{aligned}\theta_i &= 0.01091 * (i-1)\\ \phi_i &= 0.261799 * (i-1)\end{aligned}\right] 1 \leq i \leq 264 \text{ (no of samples)}$$

Step 2 Compute angular distances:

δ_{ij} = angular distance between i and j samples (Section 2.2)

Step 2A Print the distance matrix, δ_{ij} (Subroutine IADWRT), if needed:

Step 3 Compute overlap area (Subroutine OVERLAP), if needed:

$$X_{ij} = \begin{cases}\delta_{ij}/2 \sin \alpha & \text{if } \delta_{ij} < 2\alpha * 0.99\\ \delta_{ij}/2\alpha & \text{if } 2\alpha * 0.99 \leq \delta_{ij} \leq 2\alpha\end{cases}$$

O_{ij} (overlapped area - Section 2.3)

Step3A Print the overlap matrix, O_{ij}.

Data Files

There are no data files. All input is hard coded in the program.

Program Output

See Appendix A1 for the printout of an arc distance matrix
and Appendix A2 for the printout of an overlap area matrix

3.2 Optimum Sampling Program

Program Overview

This program (in PL/I) computes overlap percentages (PERCENT) of any two field-of-views (FOV) scanned by the PARABOLA predetermined value for various fields of view (ALPHA = $\frac{1}{2}$FOV) by the equations described in Section 2.3. The output will show the selected samples in sequence and overlap fractions with the next selected one.

Program Requirements

Algorithm

Step 0 Read in input data: ALPHA ($\frac{1}{2}$ FOV in radians), first value of "i" and PERCENT overlapped area (in fractions)

Step 1 Compute sensor locations:

$$\left.\begin{aligned}\theta_i &= 0.01091 * (i-1)\\ \phi_i &= 0.261799 * (i-1)\end{aligned}\right] 1 \leq i \leq 264$$

Step 2 Compute angular distances:

δ_{ij} (angular distance - Section 2.2)

Step 2A: Print the distance matrix, δ_{ij}, (Subroutine IADWRT), if needed

Step 3 Compute Overlap areas (Subroutine OVERLAP)

$$X_{ij} = \begin{cases}\delta_{ij}/2 \sin\alpha & \text{if } \delta_{ij} < 2\alpha * 0.99\\ \delta_{ij}/2\alpha & \text{if } 2\alpha * 0.99 \quad \delta_{ij} < 2\alpha\end{cases}$$

O_{ij} (overlap area - Section 2.2)

Step 4 If $O_{ij} \leq$ PERCENT and i, j $\leq$ first value of i, then output

end.

Individual Routine Descriptions

MAIN PROGRAM

This routine calculates the arc distance between any 2 pixels

Variables:

ALPHA	$1/2$ field of view (input data in radians)
TI	Theta (θ)
PI	Phi (ϕ)
ARC(264,264)	Arc distance (δ_{ij})

SUBROUTINE OVERLAP

The purpose is to calculate the overlap areas and select pixels pairs which fall in the predetermined overlap category.

Variables:

ALPHA	$1/2$ field of view
ARC (264, 264)	arc distance (δ_{ij})
PERCENT	predetermined percentage (input data in fractions)
XIJ(264,264)	intermediate variable needed to compute area
AREA (264,264)	overlap area (O_{ij})

3.3 Footprint Ground Patterns Program

Program Overview

This program (in FORTRAN) computes the off-nadir view angle and the sensor azimuth measured counterclockwise from the north horizon as well as various parameters for plotting the footprint ellipses of the PARABOLA sensor defined in Section 2.5. After calculation of the size, positions and centers of the ground patterns plotting routines are invoked.

Program Requirements

Algorithm:

Step 0 Initialization and input data

η_c = 81.2° (max nadir angle to draw footprint ellipses : SNADCR

H = 2 (sensor height - in arbitrary units)

α = 7.5° = .1309 radians (half angle of the sensor field of view) : ALPHA

PI1P5 = 4.71235 = 270° = 3 $\pi/2$

N = 360 (number of segments to draw a circumference)

π = 3.14159 : PI

Step 1 Compute sensor locations and off-nadir view angles:

θ_i = .0109083 * (i-1) : THETA

ϕ_i = .2617994 * (i-1) : PHI

$1 \leq i \leq 264$ (264 = number of pixel per run)

η_i (off-nadir view angle - Section 2.4) : SNADIR

Step 2 Proceed to the next steps if $\eta_i < \eta_c$, otherwise, go back to Step 1.

Step 3 Compute sensor azimuth and footprint ellipse parameters:

ξ_i (sensor azimuth - Section 2.4) : AZIMUR

TANALF = TAN α

TANETA = TAN η_i

a_i (half major axis - Section 2.5) : A

b_i (half minor axis - Section 2.5) : B

ℓ_c = H*TAN(η_i - α) + a_i

COSAZ = COS (ξ_i - PI1P5)

SINAZ = SIN (ξ_i - PI1P5)

$X_c = \ell_c$ * COSAZ

$Y_c = \ell_c$ * SINAZ

Step 4 Compute plotting parameters

AB = A*B

ASQ = A*A

BSQ = B*B

KL = A*N

IF (KL.LT.32) KL = 32 (arbitrarily chose 32)

IF (KL.GT.500) KL = 500 (arbitrarily chose 500)

KLAST = KL + 1

DELRAD = 6.2832/KL

ANGLE = DELRAD

Step 5 Compute points (X & Y arrays) of the ellipse

DO for K = 1, KLAST

ANGLE = ANGLE + DELRAD

SINANG = SIN(ANGLE)

COSANG = COS(ANGLE)

$$R = \frac{AB}{SQRT(ASQ * SINANG ** 2 + BSQ * COSANG **2)}$$

$X(K) = X_c + R * (COSANG * COSAZ - SINANG * SINAZ)$

$Y(K) = Y_c + R * (COSANG * SINAZ + SINANG * COSAZ)$

end do

Step 6 Plot X and Y array (an ellipse) with 'x' mark at (X_c, Y_c) and number 'i' under it if desired.

Step 7 Repeat Step 1 through 6 until i = 264

Step 8 Draw concentric circles centered at (0,0) with the radius

γ_n = H*TAN (0.2618*n)

where n = 1, 2, 3, 4, 5 with lbels 15^o, 30^o, 45^o, 60^o, 75^o

Data Files

There are no data files. All input data is hard-coded in the program.

Program Outputs

See Appendix C

Individual Routine Descriptions

The following called system subroutines are not described here. They are described in the referenced documentation manuals.

FTIO Routines (See 'IBM System/360 General I/O package')

POSN = positions to a specific file
REWIND = positions the unit specified to the beginning of the data set
CLPLTS = initializes the zeta plotter
CALPLT = invokes the zeta plotter

Wolf plotting and contouring package routines

PLOTST = initialization of all plotting levels
SETGRD = redefines boundaries of grid and object scaling
OGRID = cartesian grid overlay with tick marks
PLOT = plot data
EDIT = plots numerical value
COORD = retrieves the raster coordinates of unscaled values
HORLIN = horizontal labeling routine
CIRCL = draws a circle
FRMADV = terminates plotting of a frame and advances the frame
ENDPLT = ends plot.

MAIN PROGRAM

Purpose

This routine calculates the size, position, and centers of ellipses as well as the off-nadir angle and the azimuth, and invokes the plotting routines.

Variables:

PX(1000)	PX is the array of X coordinates of the points to be plotted
PY(1000)	PY is the array of Y coordinates of the points to be plotted
ALPHA	half field of view
RADANG	conversion factor of an angle in radians to degrees
SNADCR	maximum sensor inclination
NLOOP	number of scans per second
THETA	roll angle
PHI	elevation angle
A	ellipse major axis
B	ellipse minor axis
XC	X coordinate of ellipse center in object space
YC	Y coordinate of ellipse center in object space
XS	X coordinate of ellipse center in subject space
YS	Y coordinate of ellipse center in subject space

3.4 Sky Scanning Patterns Program

This program (in FORTRAN) computes the off-nadir view angle and the sensor azimuth as well as various parameters for plotting the sky scanning patterns described in Sections 2.7 and 2.8. After calculation of the size, positions and centers of the circular and elliptic sky patterns, plotting routines are invoked.

Program Requirements

Algorithm

Step 0 — Initialization and input data

$\eta_c = 89.9^o$ (max nadir angle) :SNADCR

H = 1.(sensor height inches)

$\alpha = 7.5^o = .1309$ radians (half angle of the sensor field of view) : ALPHA

NLOOP = 264 (number of pixels per run)

KPOINT = 121 (number of points to draw a circle or ellipse)

NCIRCL = 6 (number of concentric circles to be drawn)

RINCR = incremental radius of concentric circles

Step 1 — Compute sensor locations

$\theta_i = .0109083 * (i-1)$: THETA

$\phi_i = .2617994 * (i-1)$: PHI

$1 \leq i \leq 264$

264 = number of pixels per run

$\eta_i = \cos^{-1}(\sin\theta \sin\phi)$: SNADIR

Step 2 — Proceed to the next step if $\eta < \eta_c$

otherwise go back to Step 1

Step 3 — Compute ξ (sensor azimuth- Section 2.4) : AZIMUR

Compute X_c, Y_c (circle centers)

Step 4 Compute points (PX and PY arrays) of the ellipse sky pattern projection (Subroutine ELLIPSE)

```
A = a_i (half major axis - Section 2.8)
B = b_i (half minor axis - radius R)
COSAZ = COS(AZIMUR)
SINAZ = SIN(AZIMUR)
AB = A*B
ASQ = A*A
BSQ = B*B
KL = KPOINT - 1
DELRAD = 6.2832/KL
ANGLE = - DELRAD
KN = 0
```

Step 4A

```
DO 2  K = 1, KPOINT
ANGLE = ANGLE + DELRAD
SINANG = SIN(ANGLE)
COSANG = COS(ANGLE)
R = AB/SQRT(ASQ*SINANG**2+BSQ*COSANG**2)
X = XC + R*(COSANG * COSAZ - SINANG * SINAZ)
Y = YC + R*(COSANG * SINAZ + SINANG * COSAZ)
IF (ABS(Y) .GT. 5 GOTO 2
IF (ABS(X) .GT. 5 GOTO 2
KN = KN + 1
GOTO 2
PY(KN) = X
PY(KN) = Y
2 CONTINUE
```

Step 4B CALL PLOT (plots ellipses)

Step 4C CALL EDIT (Writes sequence numbers)

```
Step 5      Draw concentric circles
            DO 3 I = 1, NCIRCL
            R = J*RINCR
            XO=5.5 + R
            CALL CIRCLE
            CALL HORLIN
          3 CONTINUE
            END
```

Data Files

There are no data files. All input data is hard-coded in the program.

Program Outputs

See Appendix D.

Individual Routine Descriptions

The system subroutines listed in Section 3.2 are also used in this program.

MAIN PROGRAM

Purpose

This routine computes the off-nadir angle and azimuth of the sensor for each sample data and invokes the ellipse subroutine and the plotting routines.

Variables

RSIZE	radius of the largest concentric circle in inches
MAXANG	maximum angle
NDIANG	intervals of concentric circles in degrees
RADANG	conversion factor
PI	
H	sensor height
SNADCR	maximum sensor inclination angle
AZIMUR	sensor azimuth
XC	X coordinate of ellipse center in object space

YC Y coordinate of ellipse center in object space

SUBROUTINE ELLIPSE

This routine calculates the size and positions of the helical sky patterns.

Variables:

RADIUS	= F*ALPHA
SNADIR	$= \eta = \cos^{-1}(\sin\theta_i \sin\phi_i)$
AZIMUR	sensor azimuth
A	major axis
B	minor axis

BIBLIOGRAPHIC DATA SHEET

1. Report No.	2. Government Accession No.	3. Recipient's Catalog No.
TM-86171		

4. Title and Subtitle	5. Report Date
A SPHERE-SCANNING RADIOMETER FOR RAPID DIRECTIONAL MEASUREMENTS OF SKY AND GROUND RADIANCE: THE PARABOLA FIELD INSTRUMENT	November 1984
	6. Performing Organization Code
7. Author(s)	8. Performing Organization Report No.
Donald W. Deering and Peter Leone	
9. Performing Organization Name and Address	10. Work Unit No.
NASA/Goddard Space Flight Center Greenbelt, MD 20771	11. Contract or Grant No.
	13. Type of Report and Period Covered
12. Sponsoring Agency Name and Address	Technical Memorandum
	14. Sponsoring Agency Code

15. Supplementary Notes

This paper in a less comprehensive form will be submitted to the Remote Sensing of Environment Journal for refereed publication.

16. Abstract

A unique field instrument, called the PARABOLA, has been designed, along with a collapsable support boom, to be self-contained and easily transportable to remote sites to enable the acquisition of radiance data for almost the complete (4π) sky-and-ground-looking hemispheres in only 11 seconds. The PARABOLA samples in 15^0 instantaneous field-of-view sectors in three narrow-bandpass spectral channels (currently filtered for visible, near-infrared and shortwave infrared wavelengths) simultaneously. Laboratory tests and calibrations have been performed, data processing software has been developed, and instrument modifications have been made based on field use evaluation. Field measurement studies have been performed on a variety of earth surface cover types using a truck boom, a specially designed pickup truck mounting system, and a hot air balloon. In addition to the improved capability for better measurements to understand the nature of the bidirectional reflectance properties of earth cover types, the PARABOLA instrument has obvious potential for climatological and other studies requiring characterization of the distribution of diffuse solar radiation within the sky hemisphere.

17. Key Words (Selected by Author(s))	18. Distribution Statement
Bidirectional Reflectance Field Radiometer Sky Radiance Measurement Ground Radiance Measurement	

19. Security Classif. (of this report)	20. Security Classif. (of this page)	21. No. of Pages	22. Price*
Unclassified	Unclassified		

*For sale by the National Technical Information Service, Springfield, Virginia 22151.